Chemistry | Lancaster University

Electroactive hydrogels for drug delivery

MSc by research thesis.

A dissertation submitted Lancaster University for the degree of Master of Science (by research) in Chemistry.

September 2018.

Sophie Au-Yong, BSc (Hons)

STUDENT NO.: 32241861

SUPERVISOR: Dr. John G. Hardy

Declaration

No portion of the work referred to this dissertation has been submitted in support of an application for another degree qualification for this or any other university or institute of leaning.

Sophie Au-Yong

Acknowledgements

I would like to thank Dr. John G. Hardy for his supervision throughout my project on electroactive hydrogels and the department of chemistry for their support. Additionally, I want to thank Dr. Melike Firlak for her help in drug delivery and I would also like to give my thanks to Mark Ashton for synthesising PEDOT in chapter 2.

I would also like to thank my family for their encouragement as well.

Table of contents

Chapter 1: Implantable electroactive hydrogels.

Chapter 2: Injectable electroactive hydrogels

Introduction

Thesis introduction

Drug delivery systems

Pharmaceuticals have been continuously developed and explored since the discovery of biologically active compounds (as early as 2600 BC) to prolong and improve life.[1] Most people will have taken some form of medicine to relieve pain or restore the body's health at some point throughout their lifetimes. As more novel technologies are being invented, further advancements in the way that drugs can be carried/released are driving innovations in modern healthcare.

There are a few widely used ways of drug administration, namely; oral, transdermal and ocular means. Although these forms of administration provide a beneficial effect, the drug essentially gets delivered all around the body, in areas in which it is necessary as well as areas where it is not required. Whilst this is sufficient for drugs with low toxicity levels, its efficacy can be improved by targeted delivery. For example, paracetamol has relatively low toxicity as opposed to anticancer drugs (e.g. dexamethasone).[2,3] Drug delivery systems can offer an alternative approach if they are designed for localised delivery. In addition to targeted drug delivery, newer delivery systems offer the most desirable characteristic of being able to sustain release by minimising the fluctuation of the drug concentration within the body which is one of the major issues with conventional drug delivery systems (i.e. when drugs are first administered using traditional drug delivery methods (e.g. tablets, injections etc.), the concentration of drug circulating in the body will rise and then decline as it gets used/degraded/excreted). Each drug has its own therapeutic window, between a minimum therapeutic level and a maximum therapeutic level where it produces a beneficial effect (diagram 1). If concentrations fall below the minimum therapeutic level, there will be no effect on the body and if it rises above the maximum level, it can potentially be toxic and cause unwanted side effects.[4] Typically drugs administered orally have a quick release and last a short period time. Hence, it is necessary to repeat the dosage after the concentration falls to zero. The danger of this is, redosing when the concentration is already at its peak could lead to a build-up of the drug, reaching toxic concentration levels. Ideally, optimum drug delivery systems would release a specific amount of drug to a precise location of the body. They are already being currently utilised in clinical applications, in the forms of implantable or injectable devices, coatings for devices and transdermal patches. Such systems should be able to improve patient compliance due to the reduction in dosage.

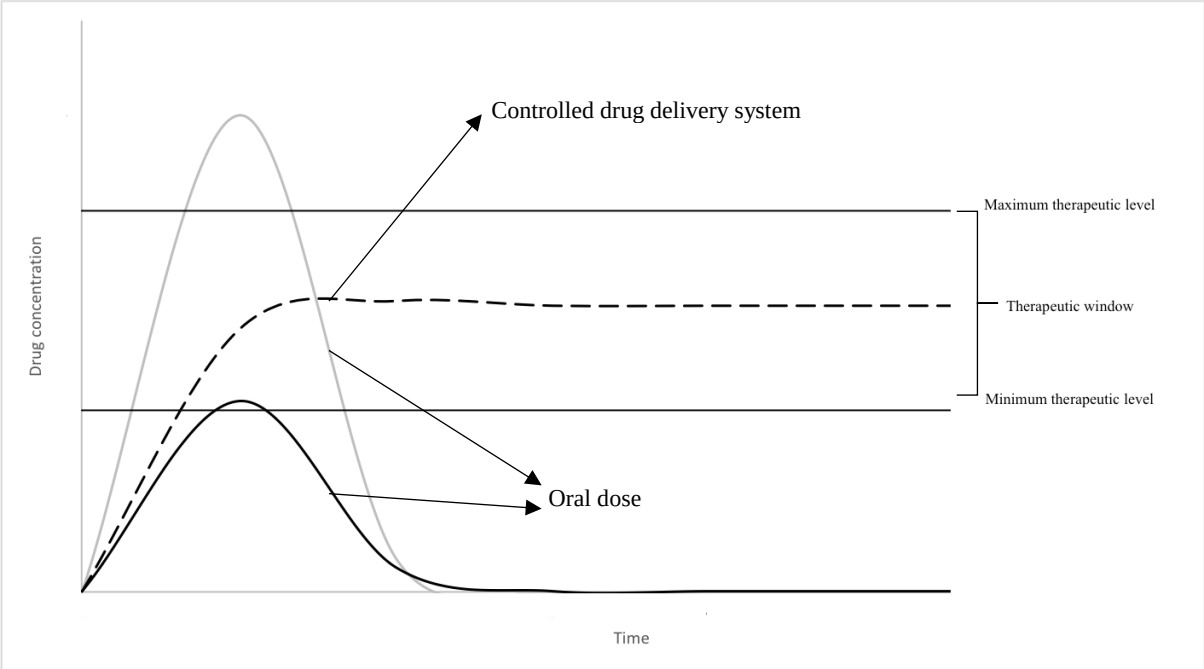

Diagram 1: Release profile of the concentration of drug after oral administration (black and grey solid) and a drug delivery system

Stimuli responsive systems

Responsive drug delivery systems can trigger release by the presence of external factors such as temperature, light, electric/magnetic fields or pH.[5–8] Such systems are capable of releasing a controlled amount of drug when desired, however the release rate of these systems are predetermined and therefore the main motivation of developing these systems is to be able to alter the concentration of drug released.[9] The use of external stimuli can mean tailored regimes for each patient and hence maximum therapeutic effect in the body from the drug will be maintained. Electrical stimuli has attracted a lot of attention due to the low costs and ease of control i.e. adjusting the release rate of drug after administration. The advantage electrical triggers have over other stimuli is the ability to finely tune the voltage applied to systems and thereby enhance the level of control.

Electroactive polymers/conducting polymers

Electroactive Polymers (EAPs) is a term used for a large class of polymers that show a change in shape or size in the presence of an electric field/current. Conducting polymers (CPs) are a class of EAPs and have potential for use in biomedical applications (e.g. neural electrodes, drug delivery systems etc.) and technical applications (e.g. light emitted diodes, LEDs). The difference being is that the electric current is typically carried along the backbone of the CPs.[10] They possess semiconducting electrical properties and can in certain circumstances be processed easily into various materials morphologies (e.g. films, fibers, foams). The synthesis of conducting polymers often requires oxidative polymerisation either

chemically in solution or electrochemically on an electrode. The conductivity of these polymers arise from their highly conjugated backbone after polymerisation. Oxidation causes positive charges to be formed along their backbone and act as sites for negatively charged molecules to interact (acting as dopants). EAPs are intrinsically semi-conductors and in terms of band theory, they will possess a relatively small band gap which allows for the partially filled valence band to promote electrons to the conduction band (diagram 2). In comparison, insulators will have a large band gap in which electrons cannot be excited to the conduction band resulting in very poor conductivity. Conductors do not have a forbidden band gap but instead have overlapping valence and conduction bands which allow electrons to readily move from the valence band into the conduction band resulting in excellent conductivity.

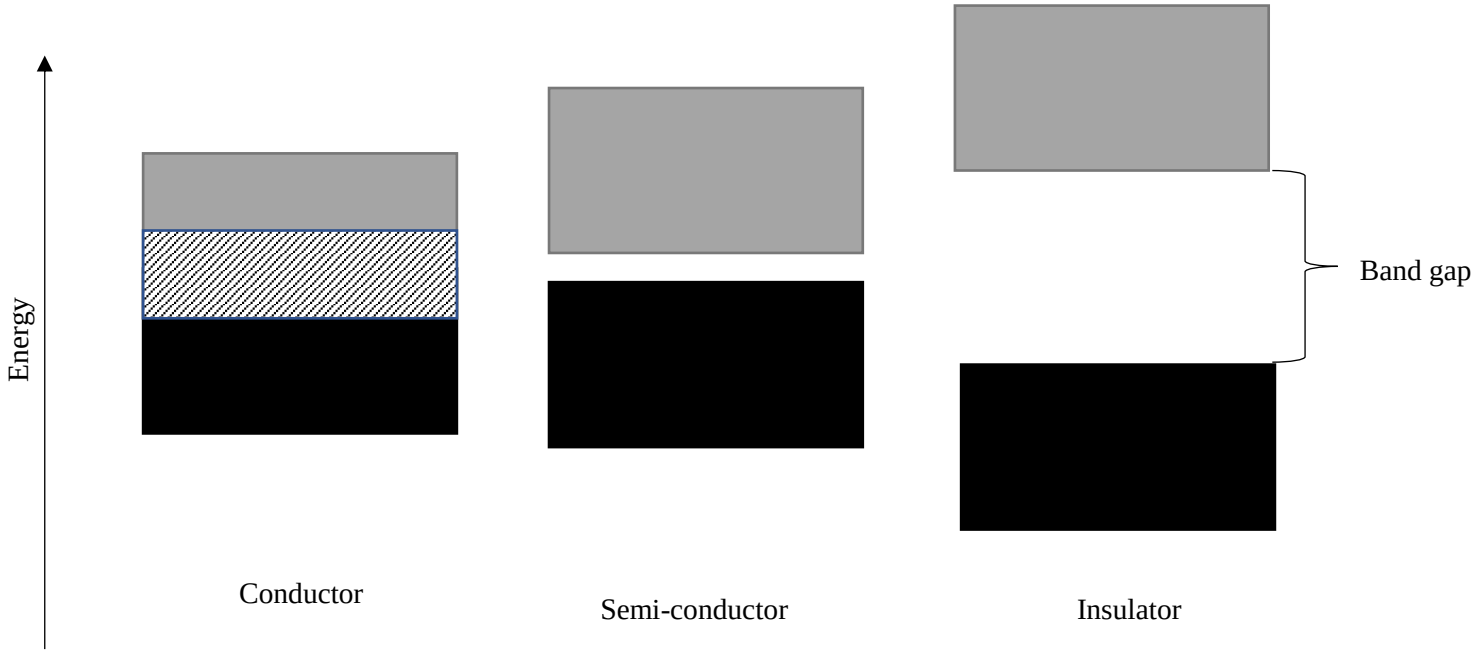

Diagram 2: Band structures for conductors, semi-conductors and insulators showing conduction band (grey) and valence band (black).

Electroactive polymers/conducting polymers in drug delivery

Hydrogels are three-dimensional polymer crosslinked materials that can be used as drug delivery systems. They are capable of swelling without being completely soluble in solvents. Typically hydrogels are not responsive however, they can be designed to be electro-responsive by the incorporation of electroactive polymers (EAPs).[11] Some examples of conducting polymers in drug delivery include polypyrrole (PPy), poly(3,4-ethylenedioxythiophene) (PEDOT) and pole(N-methyl pyrrole).[9] One of the main drawbacks of EAPs are that most have poor biodegradability. However, as newer materials are being developed and with the increased attraction responsive biomaterials have received, the need for biodegradable and biocompatible components have become extremely significant. From previous research it was found that some EAPs are biocompatible (e.g. PPy).[12] These

polymers can be rendered biodegradable through chemical modification as shown by Rivers et al by inclusion of enzyme degradable bonds such as esters.[13] One of the main challenges of designing electro-responsive drug delivery systems is that they are be known to release drug molecules in the absence of an electrical stimulus via passive leaching. For these systems to be used for drug delivery the behaviour of spontaneous drug release should be predictable and accounted for. In theory, EAPs in their oxidised forms can be doped with either opposite charges or neutral drugs in order for release.

Overview of the project

This study is based on the incorporation of EAPs into hydrogels with the aim to synthesise a novel biomaterial which is intended for use as for drug delivery devices. In the first results chapter, the idea was to synthesise partially biodegradable implantable gels using PPy to provide its conductivity. Such hydrogels could be used as coatings for medical devices and in theory it would be possible to generate degradable versions and connect the system to a degradable power source making the whole system degradable.

The second chapter of results focuses on hydrogels incorporating PEDOT derivatives and are intended for application as patient-specific drug delivery systems potentially able to be deployed via minimally invasive methods (e.g. laparoscopic deliver). The overarching aim was to electrically trigger the release of a drug from hydrogels with little to no passive release.

References

1 A. G. Atanasov, B. Waltenberger, E. M. Pferschy-Wenzig, T. Linder, C. Wawrosch, P. Uhrin, V. Temml, L. Wang, S. Schwaiger, E. H. Heiss, J. M. Rollinger, D. Schuster, J. M. Breuss, V. Bochkov, M. D. Mihovilovic, B. Kopp, R. Bauer, V. M. Dirsch and H. Stuppner, *Biotechnol. Adv.*, 2015, 33, 1582–1614.

2 R. C. Dart, A. R. Erdman, K. R. Olson, G. Christianson, A. S. Manoguerra, P. A. Chyka, E. M. Caravati, P. M. Wax, D. C. Keyes, A. D. Woolf, E. J. Scharman, L. L. Booze and W. G. Troutman, *Clin. Toxicol.*, 2006, **44**, 1–18.

3 J. Nguyen, A. Caissie, L. Zhang, L. Zeng, K. Dennis, L. Holden, F. Jon, M. Tsao, C. Danjoux, E. Barnes, A. Sahgal, C. DeAngelis and E. Chow, *J. Radiat. Oncol.*, 2013, **2**, 435–443.

4 A. T. Florence and G. W. Halbert, *Phys. Technol*, 1985, **16**, 164–176.

5 K. lin Deng, P. fei Zhang, X. bo Ren, H. bin Zhong, Y. bo Gou, L. rong Dong and Q. Li, *Front. Mater. Sci. China*, 2009, **3**, 374–379.

6 B. L. Guo, J. F. Yuan and Q. Y. Gao, *Colloids Surfaces B Biointerfaces*, 2007, **58**, 151–156.

7 C. S. Linsley and B. M. Wu, *Ther. Deliv.*, 2017, **8**, 89–107.

8 Q. Zhang, J. Liu, K. Yuan, Z. Zhang, X. Zhang and X. Fang, *Nanotechnology*, 2017, **28**, 405101.

9 D. Svirskis, J. Travas-Sejdic, A. Rodgers and S. Garg, *J. Control. Release*, 2010, **146**, 6–15.

10 P. Dubois, S. Rosset, S. Koster, J. M. Buforn, J. Stauffer, S. Mikhaïlov, M. Dadras, N. F. De Rooij and H. Shea, *Dig. Tech. Pap. - Int. Conf. Solid State Sensors Actuators Microsystems, TRANSDUCERS '05*, 2005, **2**, 2048–2051.

11 V. Pillay, T. S. Tsai, Y. E. Choonara, L. C. Du Toit, P. Kumar, G. Modi, D. Naidoo, L. K. Tomar, C. Tyagi and V. M. K. Ndesendo, *J. Biomed. Mater. Res. - Part A*, 2014, **102**, 2039–2054.

12 P. M. George, A. W. Lyckman, D. A. Lavan, A. Hegde, Y. Leung, R. Avasare, C. Testa, P. M. Alexander, R. Langer and M. Sur, *Biomaterials*, 2005, **26**, 3511–3519.

13 T. J. Rivers, T. W. Hudson and C. E. Schmidt, *Adv. Funct. Mater.*, 2002, **12**, 33–37.

Chapter 1: Implantable electroactive hydrogels

Abstract

Partially degradable electroactive hydrogels were synthesised based on chitosan, poly(ethylene)glycol and polypyrrole via a combination of photopolymerisation, and oxidative chemical polymerisation. The hydrogels were doped with lignin and chloride ions to that produced conductive gels. The chemical structure and morphology was determined by FT-IR, UV-Vis, ^{1}H NMR (solution state), ^{13}C NMR (solid state) and SEM. After confirming the successful synthesis, the swelling ratios of the gels were observed and the hydrogels were characterised using XRD, DSC, TGA and rheology. Drug delivery studies were performed by electrochemically loading pemetrexed disodium 2.5 hydrate (PEM) and measuring passive and active release via UV. PEM is a chemotherapeutic drug and FDA approved. It can be used in conjunction with other anti-cancer drugs or on its own.[1]

Introduction

The development of new and more potent drugs is coupled with significant investment in, research and development of advanced drug delivery systems for these substances. The need for new controlled release systems arises from limitations of conventional methods (e.g. creams, injections and tablets): (i) fluctuating drug concentrations, (ii) poor biodistribution and (iii) low solubility.[2] For example, after administering a drug, the concentration of drug in the blood rises rapidly, peaks and then declines due to a combination of renal clearance and the natural responses of the body to remove foreign substances. Every drug has a concentration range where it is therapeutically effective, below which it is not effective and above which it is toxic. Maintaining the drug within the therapeutic range depends on patient compliance and the medication regime, particularly in cases where regular dosage is required[3]. Current drug delivery systems are capable of maintaining maximum therapeutic efficacy for a long period of time (from days to years) and can be controlled with a single administration. They can prevent the drug from premature degradation and hence lower the dosage needed. However, constant-rate systems will be most beneficial if there is a significant difference between the levels of toxicity and effectiveness (wide therapeutic windows). The release rate of drug also tends to be pre-programmed which makes it only suitable for certain medication classes.

Conventional drug delivery systems typically lack selectivity and therefore drugs are distributed to normal cells and tissues, therefore causing unwanted side effects and reducing the effectiveness of the treatment by delivering the drug to areas where it is not needed. Typically, this effect is not very significant clinically if the toxicity is fairly low, if however the drug itself is extremely toxic, targeted delivery is imperative (e.g. anticancer drugs are typically unable to differentiate normal cells from cancerous ones, and hence no matter the rate of dosage, the effect will always be toxic). An ideal drug carrier can deliver the drug to a precise location at a precise time, which can be achieved by designing the drug carrier to be specific to a target of interest (for example receptors displayed on cell surfaces), positioning the drug carrier near the desired location or by implanting in places with low mobility thereby releasing the drug to the surrounding tissues and lowering systemic drug circulation.[4] In principle, these newer advanced drug delivery systems require less follow-up care, consequently, drugs that need to be administered quite regularly will have increased its efficacy by reducing dosage, and this in turn improves patient compliance which is can be poor amongst patients with chronic illnesses.[5]

Drugs can be formulated in hydrogels, lipids, polymeric micelles[6] and can then be released via implants, transdermal patches[7] and intravenous (IV) injections[8] in the form of rods, disks or films.[9,10] These materials often need to be washed after production to remove any unreacted monomers or initiators.[11] Hydrogels are hydrophilic three dimensional polymeric networks that have considerable potential as a material for drug delivery devices. They have the ability to hold large amounts of liquid (water or biological fluids) without disintegrating immediately and so, largely resemble biological tissues.[12,13]

The high water content can contribute to its biocompatibility due to water being a major component in humans.[11] Hydrogel-based biomaterials under development require biocompatibility, optionally biodegradability, tuneable mechanical properties and a porous structure (the latter two being dependent on the tissue niche they will be applied inside). The biological activity of drugs can be reduced before they reach the desired cells due to degradation via enzymes and low absorption rates, and a hydrogel matrix can provide a degree of protection from harsh environments.[13] The pore size distribution, along with other properties/features such as swelling ability, biocompatibility, biodegradability and mechanical strength can be altered by varying the synthetic/preparation method and chemical components.[14] There are three different types of mechanisms in which a polymeric material can release drug compounds, by diffusion (main process), chemical reactions or solvent activation. Hydrogels can be made to either be chemically stable or degradable all due to the chemical or physical interactions between the polymer chains. There are two distinct classes of hydrogels: physical and chemical. Physical hydrogels maintain their shape with molecular entanglements and/or secondary forces such as ionic bonds, whereas chemical hydrogels are held together via covalently crosslinked network. In addition to being applicable for drug delivery systems, they can also be utilised in other areas in biomedical fields such as wound dressing and scaffolds for tissue engineering.[15–18]

Hydrogels can incorporate various different components to make them externally responsive by modification of the polymers with responsive functional groups, which makes them promising for a variety of biomedical applications. The polymer networks can undergo a physicochemical change in the presence of an external stimulus such as: light,[19] heat,[20,21] pH[22] or electricity[23]. Hydrogels made from naturally occurring components tend to be biocompatible. Implantable externally responsive carriers should be inert to biological environment. Although there are benefits in using light, pH etc. here in this research electrical triggers will be investigated. Electrical stimulus provides advantages such as enhanced control, for example precise magnitude of currents, length of pulses and duration of intervals.[11] There is a growing body of scientific literature on the use of electricity for drug delivery, in vivo (iontophoresis) and dermal/transdermal (electroporation).[24,25] Since its electrical energy transforms into mechanical work, it can be also be made into devices that can form artificial muscles, sensors or film separation devices.[26]

Electroactive polymers (EAPs) are particularly interesting due to their ease of synthesis combined in hydrogels. They possess the electrical properties of semiconductors and metals as well as the ease of synthesis and excellent processability of conventional polymers. Highly conjugated backbones within the polymers are the reason for their conductivity, some examples include polyacetylene[27] and poly(paraphenylene).[28] In the 1980s it was discovered that some were compatible with biological substances, and hence polypyrrole, polythiophene, polyaniline and poly(3,4-ethylenedioxyphene) and their derivatives are now frequently explored for their potential for use in biomedical applications. With

the addition of enzyme cleavable bonds they can become biodegradable, and such biodegradable EAPs are suited to implants that require a short medication period (e.g. for drug delivery or tissue engineering) as opposed to nondegradable EAPs which are more efficient as long term solutions such as coatings for electrodes used for neural probes.[29]

Chitosan is a naturally occurring polymer and is a product of deacetylation of chitin, a polysaccharide which is the second most abundant in nature after cellulose.[30] The backbone of chitosan, contains a pendant primary amine group attached to the glucosidic residue which gives chitosan an overall positive charge.[31] The amino groups are useful for functionalization of the polymer.[32] Due to these benefits and because chitosan has widely been accepted as a biocompatible polymer (i. e. biodegradable and low toxicity), a large amount of research already exists on using chitosan as the main component for pharmaceutical purposes.[33–35] Two drawbacks of chitosan are its solubility, typically requiring a pH lower than 7 to ensure the primary amines are protonated, and therefore the solubility depends on the degree of deacetylation and its molecular weight.[36,37] Through chemical modification, the characteristics of CS can be altered potentially through the addition of other polymers. Large quantities of lignin can be found in the cell wall of plants, where it contributes to their rigidity. To use this biopolymer in biomedical applications could be advantageous due to its antibiotic, anti-fungal, anti-carcinogenic and UV-absorption abilities.[38] Yudin et al. have previously synthesised CS-lignin composites in order for tissue engineering.[39] In this study lignin is used as a reinforcing agent and dopant for polypyrrole.[40]

The key motivation of this project is to synthesise biodegradable electroactive hydrogels by using polypyrrole to give the degradable hydrogels electrical conductivity. We used a chemically modified chitosan derivative (scheme 1) to enable us to prepare hydrogels via photocrosslinking the methacrylates attached to some of the amines on chitosan and subsequently anchor polypyrrole to the backbone of the chitosan from pyrrole units attached to the amines on chitosan.[41]

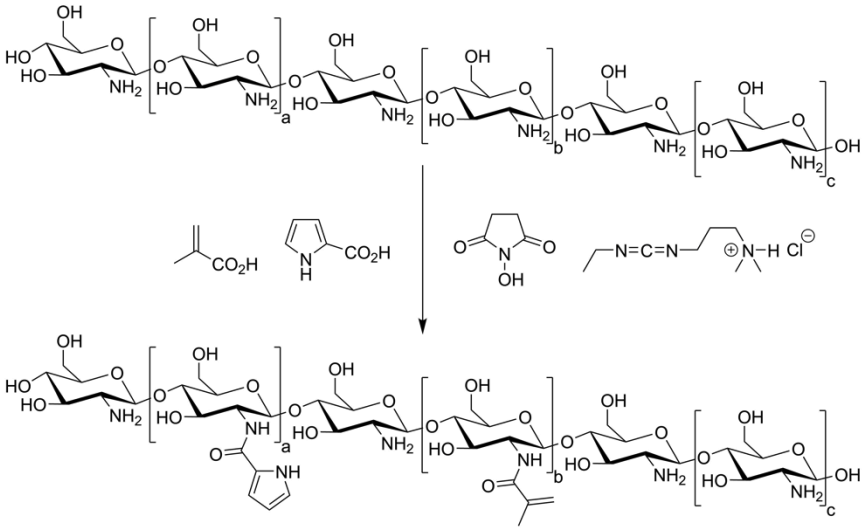

Scheme 1. Chemical modification of chitosan.

Experimental

Materials

Unless otherwise noted, all chemicals and consumables were purchased from either Sigma Aldrich or Thermo Fisher, of analytical grade, and used without further purification/modification.

Synthesis

Chitosan derivatives. (Attaching pyrrole carboxylic acid and methacrylic acid to chitosan). Chitosan (2 g, medium molecular weight) was added to water (200 mL), to which pyrrole-2-carboxylic acid (1 g, 9 mmol) and methacrylic acid (0.76 mL, 0.78 g, 9 mmol) was added and the reaction mixture andwas stirred vigorously until the chitosan dissolved. N-(3-dimethylaminopropyl)-N'-ethylcarbodiimide hydrochloride (EDC, 3.8 g, 19.8 mmol) and N-hydroxysuccinimide (NHS, 2.8 g, 19.8 mmol) were added to the solution by stirring for 24 h at room temperature in the dark.

The modified chitosan was purified by dialysis (MWCO 3500) against (DI) water for 3 days (changing the water at least 4 times per day), after which the modified chitosan was lyphophilised (Labconco freeze dryer) for 4 days. A solution of modified chitosan 0.45 wt% was stirred in DI water until homogenous and was used for formation of hydrogels.

Non-conductive hydrogels (photopolymerisation). The photoinitator- 2-hydroxy-4'-(2-hydroxyethoxy)-2-methylpropiophenone (Irgacure-I2959) 0.1 wt% was added to the chitosan derivative solution; and poly(ethylene) glycol diacrylate (PEGDA, Mn 2000) was added at a concentration of 5 mg per 100 μL. This mixture was stirred in the dark for ca. 2 until homogenous.

Silicone isolators (molds) produced by Grace Bio-Labs (Sigma Aldrich) (9 mm in diameter x 0.8 mm in depth) were placed onto glass slides after removing dust particles using tape. 75 μL of solution was injected into each well. The glass slides were then transferred into petri dishes and irradiated for 1 h under a Mega LV202E UV exposure unit (with 2 x 8W bulbs, output from ~ 300-460 nm, peak at 365 nm). The reaction mixture was left in the molds to allow the reaction to complete overnight.

Conductive hydrogels (doping with lignin and pyrrole). Irgacure-I2959 (0.1 wt%) and PEGDA (at the concentration of 5 mg per 100 μL was added to modified chitosan solution, and the mixture was stirred until homogenous. Pyrrole (200 μL, 4.3 mmol per mL of PEGDA-modified CS) was purified by passage through an alumina column added to 1 mL of PEGDA-modified chitosan with lignin (lignin alkali, low sulfonate content, 100 mg/mL) and left to stir at room temperature until homogenous.

This solution was then pipetted into silicon isolators (Sigma Aldrich), 75 μL in each well. Reaction mixtures were photopolymerised for an hour and left over night for complete reaction.

Following UV radiation, ferric chloride (1 wt%) was dissolved in water and the gels were left to incubate for 24 hours. Afterwards, the supernatant was decanted. The samples were then washed thoroughly with water until the water became clear and colourless and left in DI water for 24 hours.

All hydrogel samples were kept in the petri dishes along with a moist kimwipe wrapped in parafilm, to prevent the gels from drying out.

	Non-conductive	**Conductive**
Water	1 mL	1 mL
Modified chitosan	4.5 mg	4.5 mg
Igracure-I2959	1 mg	1 mg
PEGDA	50 mg	50 mg
Lignin	N/A	100 mg
Pyrrole	N/A	200 μL

Table 1. Table showing the composition of each hydrogel reaction mixture.

Characterisation

UV-Vis spectroscopy. Tested on Thermo Scientific NanoDrop 2000. Solutions (3 μL) were pipetted onto the optical measurement surface/pedestal. Chitosan was dissolved in an aqueous solution of acetic acid (1 % Vol/Vol) whereas the other samples were in water.

Fourier transform infrared spectroscopy in attenuated total reflectance mode (FTIR-ATR). An Agilent Technologies Infrared Spectrometer was used to record spectra in ATR mode in the range from 4000-500 cm^{-1}. The data was exported to ResPro and the baseline was corrected.

Solution state proton NMR spectroscopy. ^{1}H NMR spectra were recorded with a Bruker AVANCE III 400 (NanoBay) equipped with a 5 mm ^{1}H-X broadband observe (BBO, 109Ag-19F) RT probe.

(3-Trimethylsilyl)propionic-2,2,3,3-d_4)) was added as a reference in all samples): 1 mg of chitosan medium MW was dissolved in 1 mL of 2% DCl vol/vol (35 wt% in D_2O) in D_2O solution and heated to ~70°C for an hour or until complete dissolution. For modified chitosan, the same procedure was followed however heating was not necessary. Acetic acid was dissolved in D_2O at a concentration of (5 mg/mL). Pyrrole-2-carboxylic acid was dissolved in DMSO-d_6 at a concentration of (5 mg/mL). The spectra of methacrylic acid was acquired in both D_2O and DMSO-d_6.

Each of the solutions were then pipetted into 5 mm NMR tubes (Sigma Aldrich, Norell standarad series 5) and inserted into the NMR.

Solid state ^{13}C NMR. Bruker AVANCE III HD 700 WB was used to observe cross-polarization/magic angle spinning of the samples.

X-ray diffraction. XRD patterns were investigated using a Rigaku SmartLab powder diffractometer in a 2θ with a scattering range of 5 to 40° and a resolution of 0.1°.

Differential Scanning Calorimetry (DSC). Thermal properties were investigated with a Mettler Toledo DSC1 SOP, temperature ranging between -40 and 400°C. Approximately 5 mg of sample was sealed in a hermetic aluminium pan (40 μL).

Thermogravimetric Analysis (TGA). Thermal stability of vacuum dried hydrogels (ca. 4-5 mg) were observed with a NETZSCH STA 449 F3 Jupiter thermal analyser. Temperatures observed were from 25 to 550°C with a heating rate of 10°C/min. The reference pan used was alumina.

Rheological characterization. Rheological properties were found using an Anton Paar Physica MCR 302 rheometer fitted with a parallel plate with a diameter of 12.484 mm. Strain sweep experiments were employed with a constant frequency of 10 rad/s. Frequency sweeps were performed at 0.5% strain for non-conductive hydrogels and at 0.1% for conductive hydrogels.

Swelling studies. The swelling ratio of the hydrogels was determined by recording the initial mass its dry state (m_0) and the mass after swelling in PBS for 24 hours (after removal of excess water by wicking with filter paper). Swelling behaviour was observed at room temperature and calculated using the following equation where m_t is the mass at the time t and m_0 represents the initial mass.

$$Swelling\ Ratio\ (\%) = \frac{(m_t - m_0)}{m_0} \times 100$$

Scanning Electron Microscope (SEM). Morphologies of the hydrogels were captured with a JEOL JSM-7800F field emission SEM under argon atmosphere. Samples were swelled in water before freeze-drying and gold coated by a Quorum 150R ES.

Drug delivery studies: drug loading. Conductive hydrogels were electrochemically loaded with pemetrexed (using an aqueous solution of 4 mL of 1 mM pemetrexed disodium 2.5 hydrate as the electrolyte bath). The hydrogels were secured on glassy carbon electrodes by the electrode lid with a hole cut out at the top (image 1). A 3 electrode cell was composed of Ag/AgCl reference electrode, platinum mesh counter electrode and a glassy carbon electrode with the hydrogel. For 30 minutes, voltage was applied at 0.6 V via chronoamperometry. 10 μL of the solution after drug loading was diluted down 4 times with distilled water and frozen for storage prior to UV-Vis measurements. Between each measurement the electrodes and cell, were washed thoroughly.

Drug delivery studies: drug release. For stimulated drug release, the drug was released at -0.6 V in 4 mL of PBS for 30 seconds every 10 minutes 3 times. At each time interval, 10 μL of the solution was frozen for storage piror to UV-Vis spectroscopy. Passive release of the drug was carried out by placing the electrodes with hydrogels in 4 mL PBS and 10 μL samples were taken every 11 minutes in line with the sampling frequency for the samples that were electrically stimulated. To test the concentration of

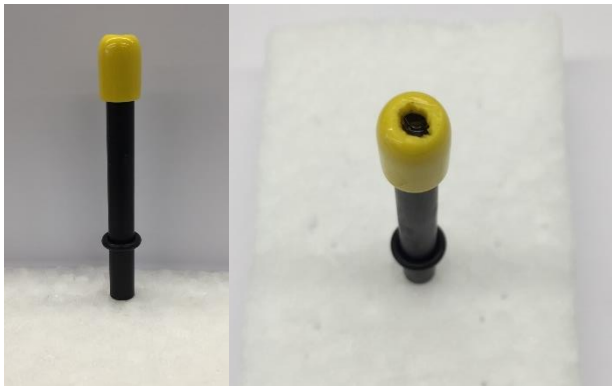

Image 1. Side view (left) and top view (right) of set up for securing hydrogels on glass carbon electrodes for drug delivery studies.

drug that was released, UV measurements were also performed on the PBS at the absorbance maximum of 225 nm which correlates to PEM.

Results and Discussion

Synthesis of CS-Py-Methacrylates / PEGDA / Lignin

A method of synthesising partially biodegradable electroactive hydrogels composed of mainly chitosan, PEGDA and polypyrrole was developed. To ensure the gels were robust to handling, the chemically modified chitosan derivative was combined with polyethylene glycol diacrylate (PEGDA) displaying polymerizable acrylate units at the termini of the polymer[42] via photopolymerisation.[43].

The backbone of chitosan contains reactive amine groups which are relatively easy to modify. Methacrylic acid and pyrrole carboxylic acid were conjugated to the chitosan using water soluble carbodiimide chemistry. Amide bonds are degradable by enzymes within the body e.g. proteases.[44] PEGDA is a common component of hydrogels because it is highly hydrophilic and biologically inert.[45] Hydrogels were synthesised via UV mediated photopolymerisation using, Igracure 2959 as the photoinitaor (which fragments into an alcohol radical whereas in the propagation step, the radical attacks the carbon-carbon double bonds (C=C) present in the methacrylates and PEGDA leading to crosslinked polymer structures) (scheme 2).

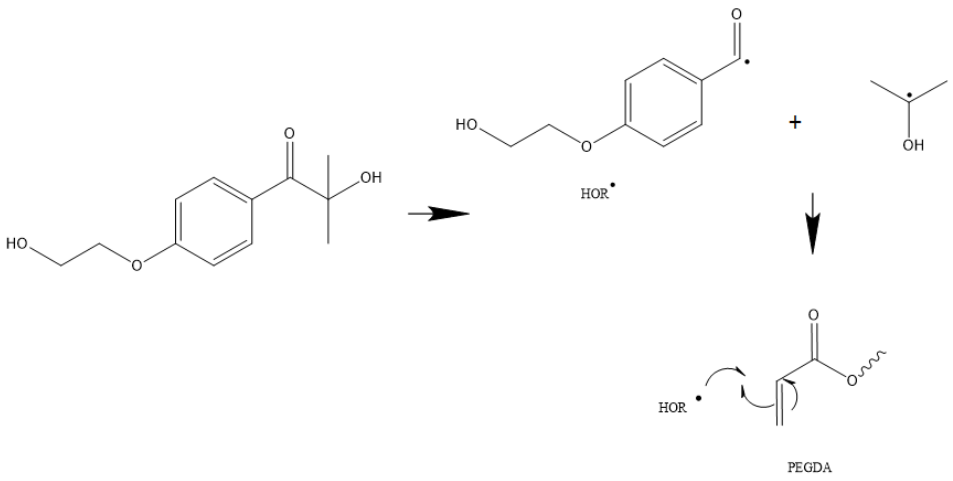

Scheme 2. Reaction scheme of Irgacure initiation and propagation step applicable to acrylates and methacrylates.

Blending chitosan and lignin may result in the formation a polyelectrolyte complex (PEC) which is a result of two oppositely charged polymers interacting ionically, where chitosan is cationic and lignin is anionic, however aggregates were not evident, potentially due to the presence of pyrrole which would also bind to the anionic moieties on lignin.

The electroactive and conductive polypyrrole forms an interpenetrating network in the hydrogel matrix by submerging the photocrosslinked hydrogels in an aqueous solution of $FeCl_3$, and the polypyrrole is doped with both lignin and chloride anions.[46]

UV-Vis spectrometry. After lyphophilisation of modified chitosan, the product was pale pink indicating a chemical reaction has happened. Figure 1 shows the UV absorption spectra of chitosan, modified chitosan, pyrrole carboxylic acid and methacrylic acid. The difference between the spectra can be identified. The absorbance present for modified chitosan is a broad peak at around 195 nm. Chitosan has a maxima of 218 mm. They show absorbances around 200 nm as chitosan contains UV chromophoric groups, *N*-acetylglucosamine (GluNAc) and glucosamine (GlcN).[47] Two peaks at ~200 and 255 nm are present in modified chitosan which are not present in chitosan which are attributed to methacrylic acid and pyrrole carboxylic acid respectively.

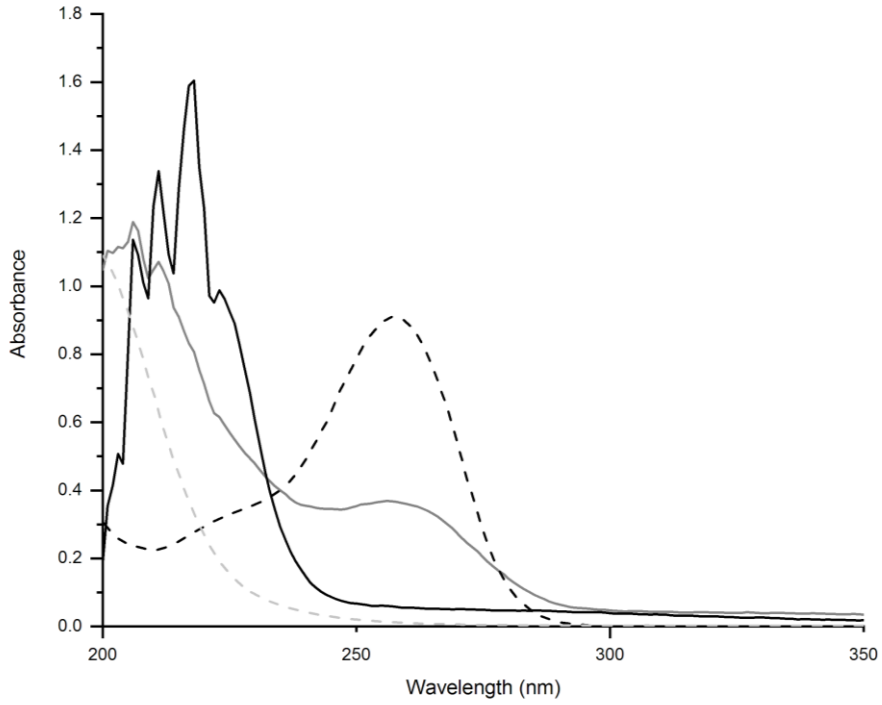

Figure 1. UV-Vis spectra of chitosan (solid black line), modified chitosan (grey line), pyrrole carboxylic acid (black dashed) and methacrylic acid (grey dashed).

FTIR – ATR mode. The FTIR spectra for chitosan (75-85% deacetylated) and the modified chitosan are shown in figure 2. Chitosan shows a broad peak at 3354 cm^{-1} which corresponds to -OH stretch overlapping $-NH_2$ symmetric and asymmetric stretch bands. The absorbance at 1566 cm^{-1} is the N-H bend of an amine group. The peak at 1149 cm^{-1} is characteristic of C-O-C ether present in the backbone of chitosan. Multiple low intensity peaks at 1419, 1373, 1321 $cm^{-1}$are ascribed to C-H bending and C-H stretching vibrations are at 2088 cm^{-1}. Sharp absorbances at 1020, 1057 cm^{-1} are C-O stretches in the alcohol groups.

Amide I (C=O stretch) and amide II (N-H bend, C-N stretch) vibrations can be assigned to peaks occurring at 1649, 1527 cm^{-1}, respectively. The intensity of the peaks responsible for C-H bending and stretching have also increased indicating methacrylate units are present. Further evidence suggesting successful synthesis of methacrylate constituents onto chitosan come from the spectra of methacrylic acid where there are absorbances at 2929 cm^{-1} and in modified chitosan spectra there is a peak at 2923 cm^{-1} from CH. Sharp absorbances in the non-conductive gels come from PEGDA, the smoothness of the conductive hydrogels suggest that the polymer networks have crosslinked with PEGDA more.

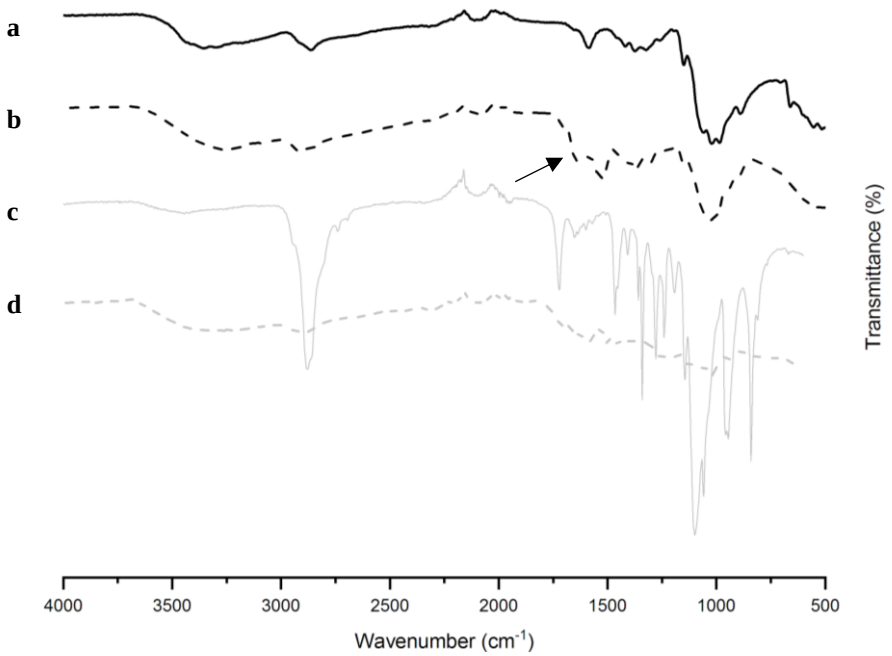

Figure 2. FTIR spectra of (a) chitosan medium molecular weight (black solid) (b) modified chitosan (black dashed): (c) non-conductive hydrogel (grey solid) (d) conductive hydrogel (grey dashed) .

Solution State ^1H NMR. NMR spectra for chitosan and chitosan derivative in DCl/D_2O are shown in figures 3. Small peak around 2.03 ppm comes from the methyl group ($-CH_3$) attached to the N-alkylated

GlcN residue. At 3.10 ppm a singlet represents H2, multiplet signals from 3.5 to 4 ppm are assigned to H3, H4, H5 and H6 of GlN. From literature, typically the spectra would show a small peak around 4.28 ppm due to H1 of both GlN and acetylated form.[48,49] Peaks from H2-H6 (~3 to 4 ppm) were integrated to approximately 600 to account for 6 protons. This results in the peak at 2.03 ppm to give a value of 73.47. From these values, the deacetylation can be calculated due to chitosan being the partially deacetylated derivative of chitin.

$$\frac{74}{600} \times 100 = \sim 12\ \%$$

Therefore the chitosan used is around 88 % deacetylated.

The spectra for modified chitosan shows new chemical shifts corresponding to the new functionality installed. The peak at 1.9 ppm is characteristic of the methyl group attached to the methacrylate (confirmed by the NMR spectra of methacrylic acid showing a peak at 1.9 ppm). Signals from ~5 to 6.5 ppm are assigned to the two protons connected to the double bond. Here, if the same peaks from chitosan are integrated again to 600 the number of protons can be determined. Peaks around 1.9 ppm are calculated to be ca. 71 and within the range of 5-6.5 ppm it is ca. 52 (the correct ratio for the methacrylate installed). A multiplet of peaks with low intensity can be seen between 7.9 and 8.1 ppm which is characteristic of pyrrole that has been attached to the backbone of chitosan (albeit very difficult to integrate in comparison to methacrylate moieties). Two-dimensional ^{1}H – ^{1}H COSY NMR links methacrylate olefins (5.5-6 ppm) to methyl at 1.9 ppm (fig. 4).

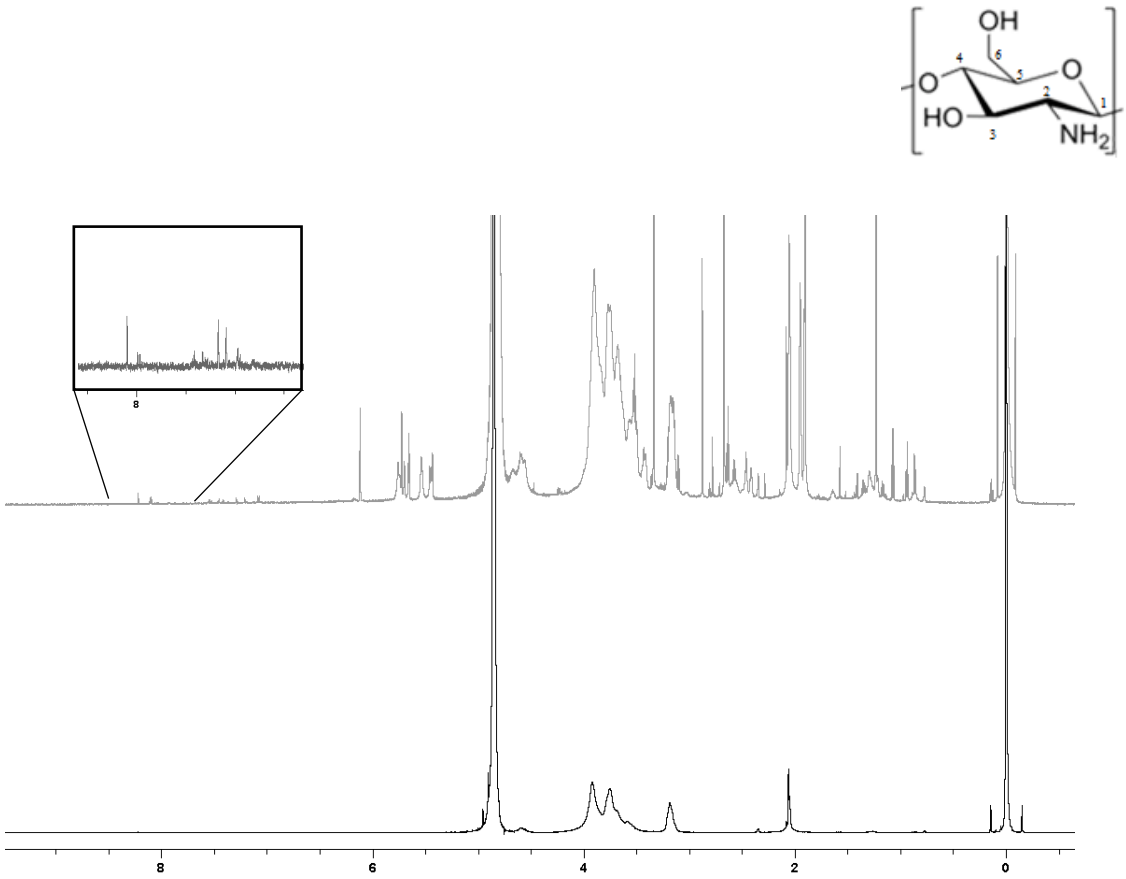

Figure 3. ^{1}H solution state NMR spectra of (a) modified chitosan (b) chitosan medium molecular weight, black.

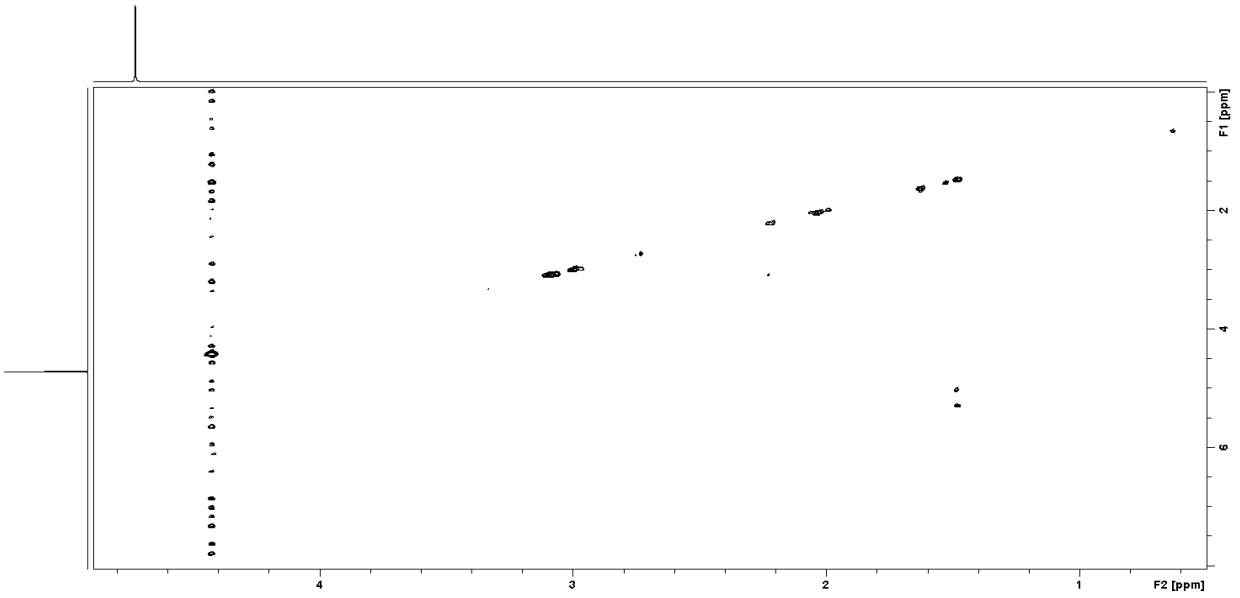

Figure 4. ^{1}H-^{1}H COSY solution state NMR spectra of (b) modified chitosan.

Solid State ^{13}C NMR. CP-MAS spectra of chitosan was recorded in its powder form supplied by Sigma Aldrich, the chemical shift assignment can be found in the literature (fig. 5a).[50,51] Modified chitosan exhibit similar shifts to chitosan, signals at 105, 83, 75, 61 and 58 ppm correspond to C1, C4, C3, C6, C2 (fig. 5b). The peaks responsible in both spectra corresponding to C=O and CH_3 (due to partial deacetylation and amide) appears at 174 and 24 ppm accordingly. Further could correlate to conjugated pyrrole in line with the literature for polypyrrole (α-carbon) to be approximately 125 ppm which appears on the spectra for chitosan derivative, β-carbon appeared at ~105 ppm and thus a small peak at 109 ppm is seen on the spectra obtained.[52] Previous research by Forsyth et al. explains the low frequency shoulder on the peak at 123 ppm exists due to β-carbons being partially oxidised as opposed to pure pyrrole.[53]

Similar absorbances for methacrylate units can also be identified from past work.[54] At 19 ppm, this signal could be due to CH_3, and at 37 ppm is possibly from C-C tertiary carbons (above the polymer chain). Alkene functional group typically shows resolution between 105-145 ppm, therefore the peak at 140 ppm was assigned to C=C.

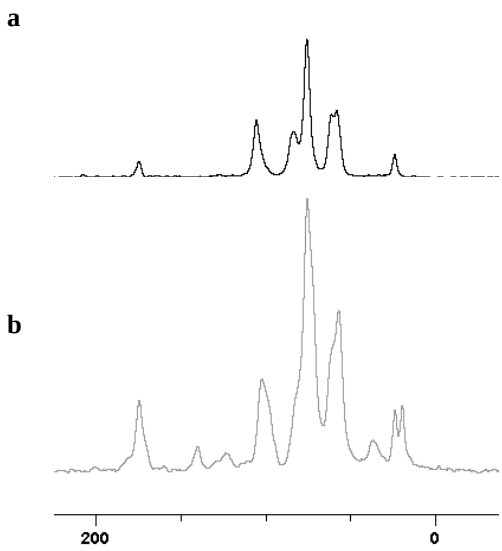

Figure 5. ^{13}C solid state NMR spectra of (a) chitosan medium molecular weight (black) and (b) modified chitosan (grey).

X-ray Diffraction. XRD patterns of the non-conductive (PEGDA/CS) gels and conductive (Py-lig-PEGDA/CS) gels were studied from 5-40° in 2θ range using XRD (fig. 6). Chitosan usually shows peaks at around 10.3°, 15.9° and 20.1°.[48] After photopolymerisation of PEGDA and modified chitosan, the curve showed no sharp peaks indicating crystallinity were present because the chitosan was dispersed in the polymer matrix. The peak obtained from non-conductive hydrogels was broad and smooth at 24.6° suggesting formation inter- and extra- molecular bonding was inferred.[48,49] From the smoothness and broadness of the peaks, it can be said that the materials are amorphous.

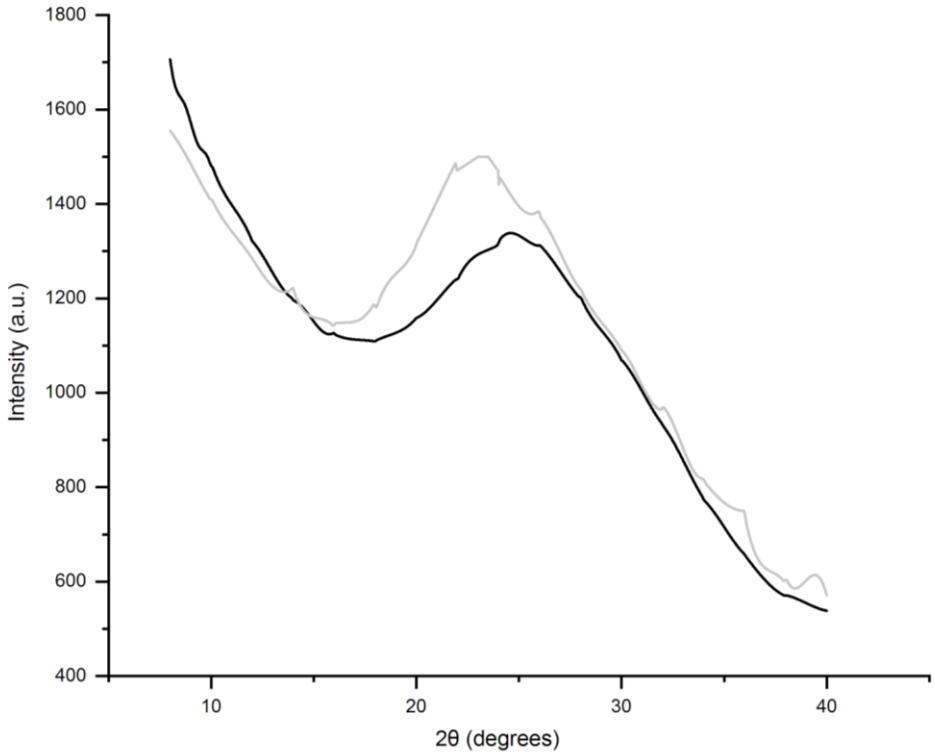

Figure 6. X-ray diffractograms of non-conductive, (grey line) and conductive hydrogels, (black line).

Differential Scanning Calorimetry. DSC curves for both conductive and non-conductive hydrogels are shown in figure 7, with the same temperature range and heating rates. The glass transition temperature of chitosan is typically around 110-117°C. On the data obtained for the conductive hydrogels a peak occurs at 120°C showing similar values to Dhawade et al.[55] Although there are similar values being shown the peak is fairly sharp compared to conventional Tg curves so another possible explanation for this peak is that it could also attributed to evaporation of residual bound water. The Tg for non-conductive PEGDA-CS copolymerised hydrogels were not detected. DSC curves for pure chitosan can be found in past papers, with the exothermic peaks for the decomposition of amine groups in chitosan at around 295°C.[56,57] For non-conductive hydrogels, this peak was observed at 288°C. Whereas for the conductive hydrogels the onset of the decomposition of was at 365°C suggesting the interpenetrating network formed after synthesis rendered them more thermally stable. Before the addition of lignin and pyrrole, hydrogels showed a peak at 50°C which is most likely due to the evaporation of water. Literature of major peaks of PEGDA was found to be at around 148°C[58], and for lignin at ~110°C[59]. Distinctive peaks on conductive gels appear at 153°C and are significantly lower than of pure chitosan itself and closer in value to PEGDA and lignin. This could be due to modification performed on chitosan, or it could suggest that PEGDA and lignin occupy a larger amount of the hydrogels. The

temperature contrast between the two hydrogels suggest the components added to make them conductive increases its thermal stability.

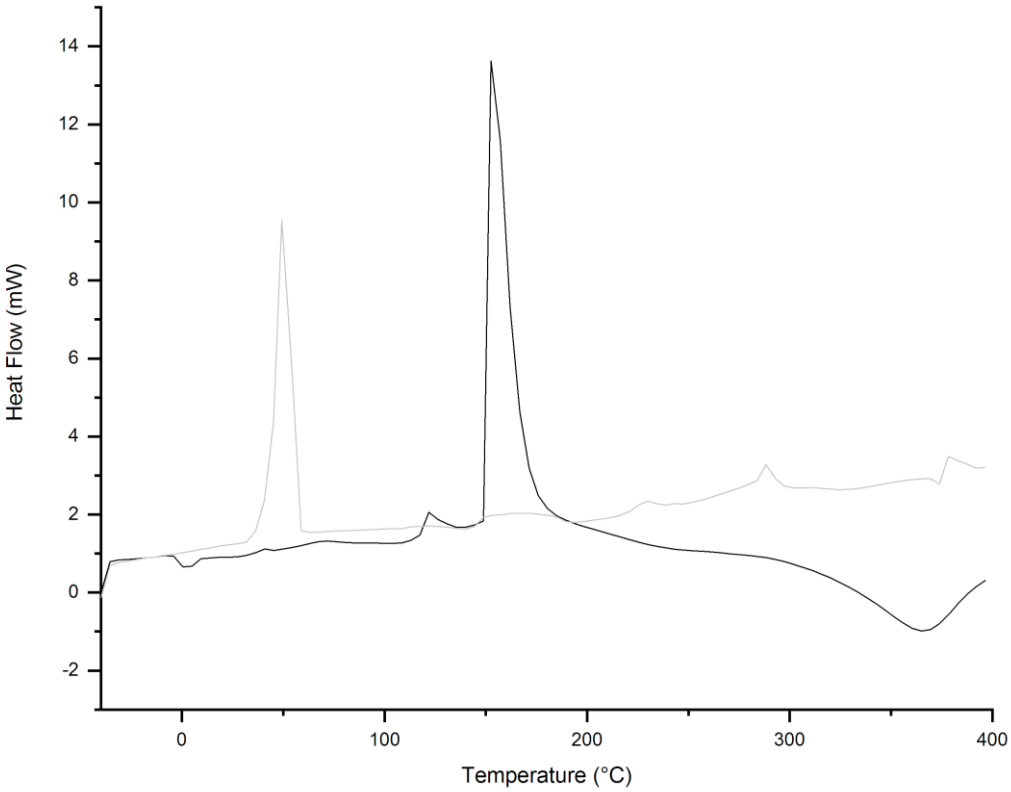

Figure 7. DSC thermograms of non-conductive hydrogels (grey) and conductive hydrogels (black).

Thermogravimetric Analysis. The thermograms of the two hydrogels are shown in figure 8. Non-conductive hydrogels showed its degradation in two distinct stages. The first signs of weight loss is a very small amount of ~5% from 45-160°C can be ascribed to volatile products with low molecular mass and is most likely to be bound water molecules. Major weight loss of about 69% occurred between 220°C and 380°C and is attributed to degradation of the polysaccharide.[60] Comparing the values to the ones obtained by Corazzari et al. it was found that chitosan has a major decomposition around 300°C.[61] The significant difference between the two values can be explained by the disruption of hydrogen bonding causing them to be weakened between chitosan chains and therefore confirms successful photopolymerisation between PEGDA and chitosan.

The thermal stability of the conductive hydrogels showed degradation in three steps. From 40-120°C evaporation of entrapped water and small volatile molecules could be represented by 8% of weight loss. The second degradation stage happens between 150°C and 402°C corresponding to the gradual loss of PEGDA with 30% drop in weight.[48] The final major weight loss of 50% is likely attributed to the decomposition of chitosan, polypyrrole and lignin at 410°C.

From TGA, it can be seen that conductive hydrogels have a higher decomposition temperature at 410°C whereas non-conductive ones occur at 220°C. The rate at which the mass decreases for gels incorporated with lignin and pyrrole is also slower than PEGDA alone. Thus, the interpenetrating network synthesised in the conductive gels can be said to provide an increased thermal stability.

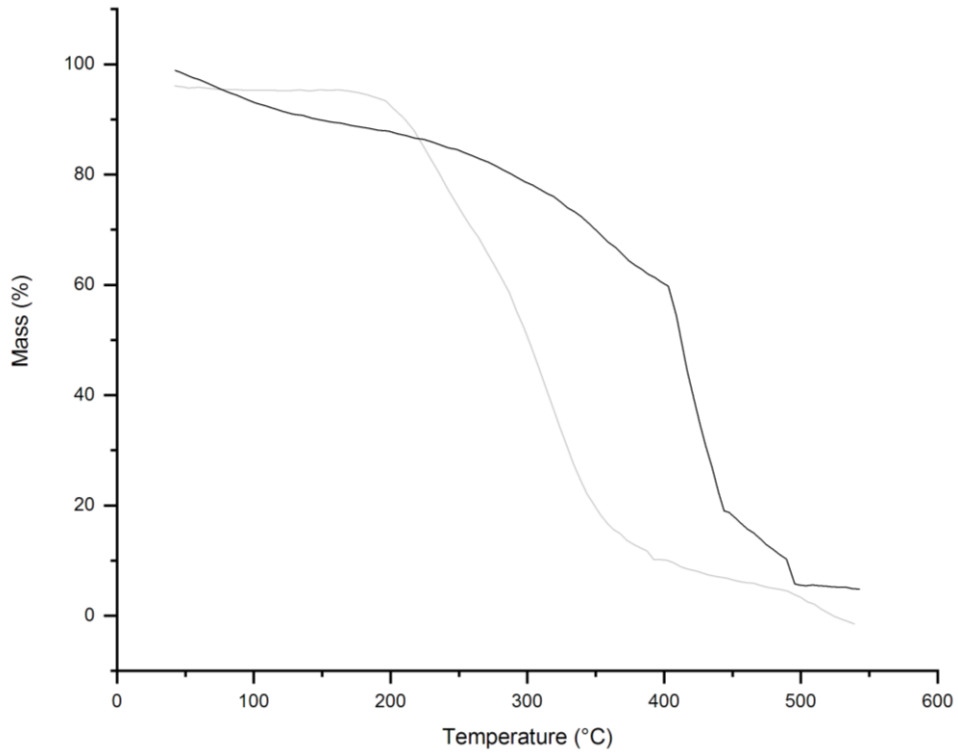

Figure 8. TGA thermograms of non-conductive hydrogels (grey) and conductive hydrogels (black).

Rheological properties. Both dynamic strain sweep and frequency sweep were performed to characterise the rheological properties of the hydrogels. Strain sweep tests were carried out at a constant frequency of 1 Hz, its storage modulus (G' – elastic) and its loss modulus (G" – viscous) at a range of different strains are shown in figure 9a and 10a. When G' is higher than G'' it suggests that the hydrogel is highly structured and the material behaves more solid-like. The point where both moduli intersect signifies the breaking point of the hydrogels and is known as the critical strain level or gel point. In the non-conductive hydrogels (fig. 9a) the critical level is around 2%, below this level indicates the gel structure is still unbroken. As strain increases past the critical level, the network bonds start to break

and the moduli both start to decline. Here, G' drops below G" showing that the hydrogel becomes progressively more liquid-like. The conductive hydrogels (fig. 10a) have a longer Liner Viscoeleastic Region (LVR) as its critical strain level is approximately 0.5%, four times lower than non-conductive hydrogels showing that the conductive hydrogels are more rheologically stable, potentially due to the additional polymer networks formed between chitosan and lignin. If no LVR exists, the gel may be considered a weak gel and hence, the non-conductive gels seem to be more elastic. Furthermore, as the values of the moduli increase along the y-axis, indicates the strength of the gel. Conductive hydrogels appear twice as strong as the non-conductive hydrogels.

A characteristic feature seen in the data points is the increase of the loss modulus (G") before the gel point. The peak represents a relaxation in the gel structure and depending on the class of soft material there are different explanations of what could have been responsible for the rise in G".[62]

Frequency sweep experiments were carried out to test the dependence of frequency to the moduli and are shown in figure 9b and 10b. The reason for performing frequency dependence tests is materials can appear to be solid-like (G' > G") in a short period of time (high frequency) but act more fluid-like (G" > G') in longer timescales (low frequency). In both frequency sweeps G' is higher than G'' confirming that the hydrogels behave more like a solid.

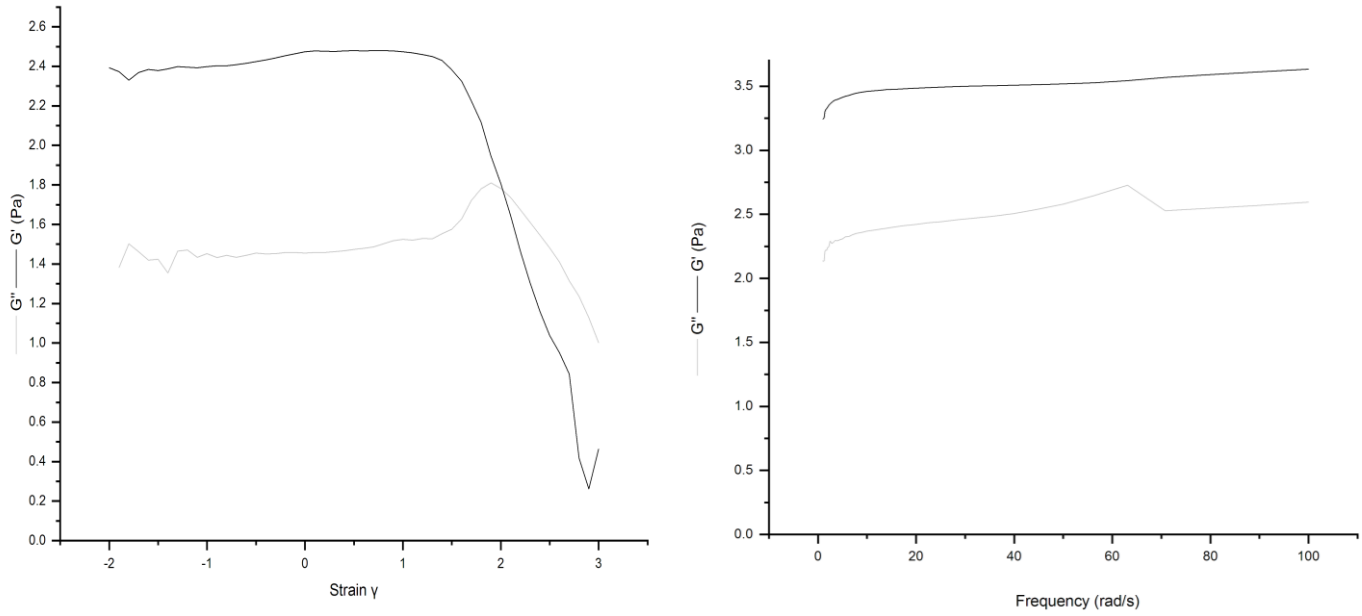

Figure 9. Rheology a) strain sweep (left) and b) frequency sweep (right) of non-conductive hydrogels.

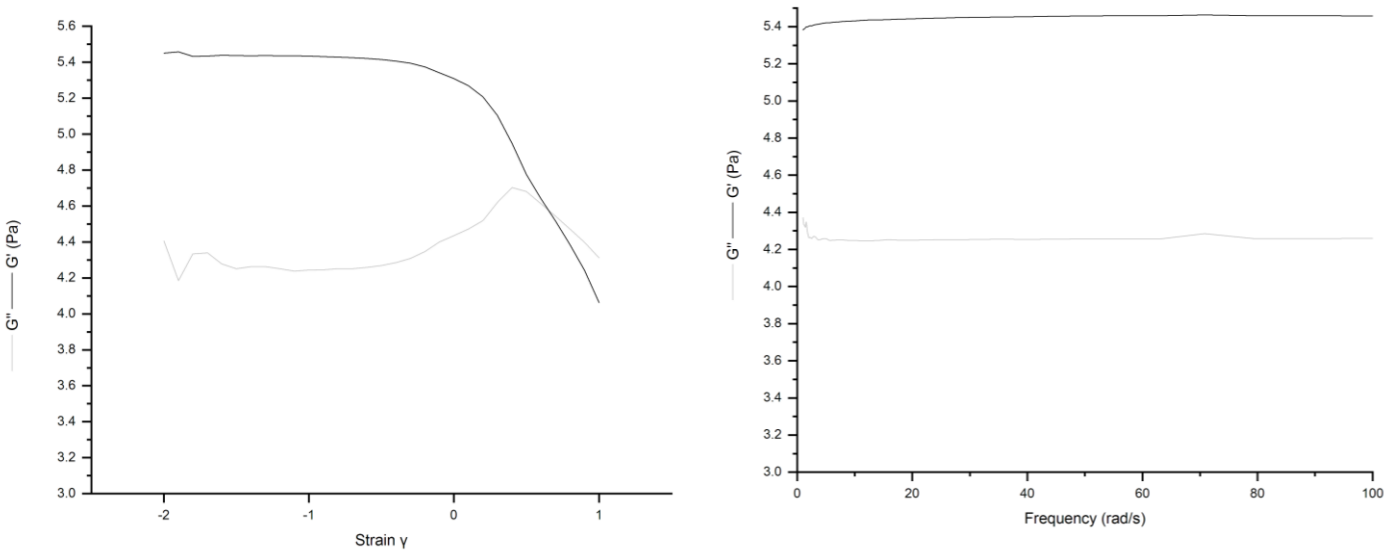

Figure 10. Rheology a) strain sweep (left) and b) frequency sweep (right) of conductive hydrogels.

Swelling studies. Hydrogels were swelled with PBS because this is a physiologically relevant buffer. The swelling behaviour of hydrogels is dependent on both the crosslinking density of the networks and the pH of the solution.[63] The conductive hydrogels were found to have a swelling ratio of 70.22% and on the other hand non-conductive hydrogels had a swelling ratio of 25.4%. Although just by appearances non-conductive gels seemed to have swell more than conductive gels a feasible explanation for the significant difference between the two can be seen in their morphology. The conductive hydrogels have smaller pores on the surface allowing for an increase of water molecules to absorb into the water. Despite the swelling ratio being higher than the non-conductive gels, compared to some hydrogels in literature it could be seen as fairly low. An increase in lignin content will decrease the swelling ability of the hydrogel due to its hydrophobicity, repelling water.[64]

Scanning Electron Microscopy. Morphology of the hydrogels can be seen in low and high magnifications displayed in figure 11 and 12-13 respectively. It can be stated that the surface of the hydrogels do not resemble the internal structure. The conductive hydrogels, as well as appearing to having a fairly smooth surface, it appears to have string-like structures extending through the surface (fig. 11b). This could have possibly arose from the polymerisation of polypyrrole. Its cross sectional area can be observed through the cracks of the surface (fig. 12), displaying many particles throughout the hydrogel matrix suggesting the presence of chitosan/lignin granules.[40] The surface of these hydrogels also exhibits very small pores dispersed quite evenly whereas non-conductive hydrogels

show slightly larger pores however are rarely present. Ji et al. reported that an increase in lignin content can decrease the average pore diameter.[64]

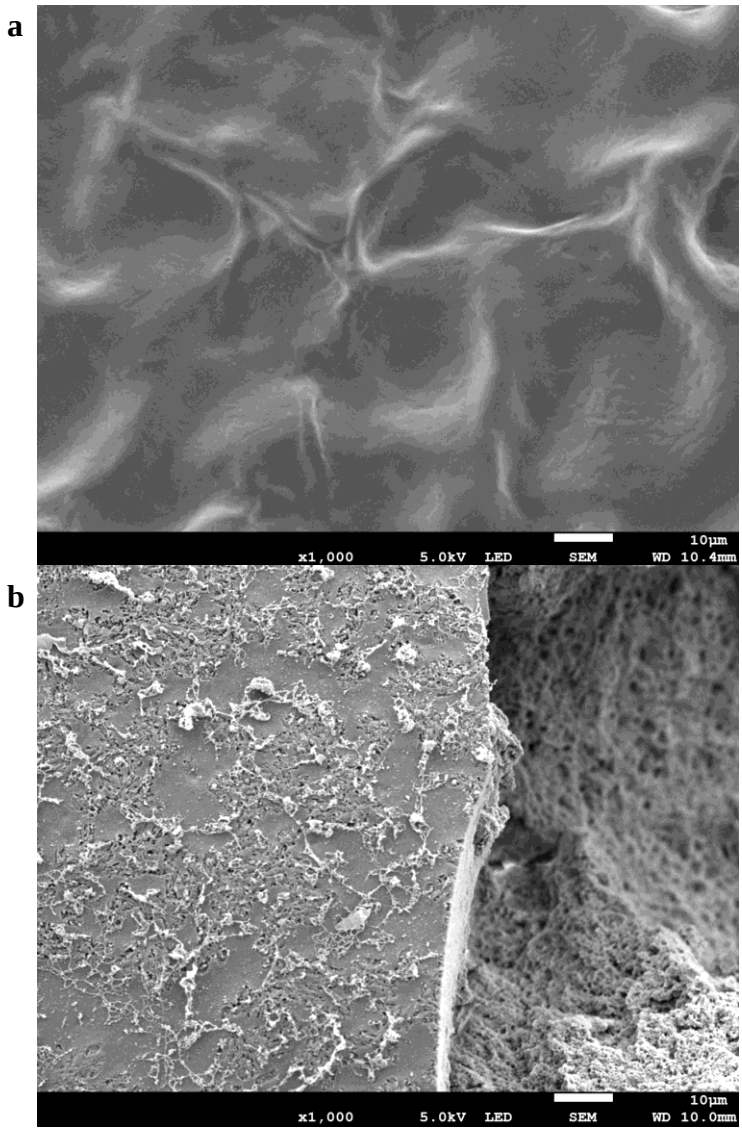

Figure 11. Morphology x1,000 magnification of (a) non-conductive (top) and (b) conductive hydrogels (bottom).

Whilst the surface of the non-conductive gels are smooth, there is evidence of probable crosslinking from the bumps. Features of surfaces can affect the rate at which the hydrogel swells. As the surface of the hydrogels become smoother the swelling rate will decrease as it becomes more difficult for water molecules to penetrate the surface, hence why the conductive hydrogels were able to swell about 30 times the amount of the non-conductive hydrogels. It is also evident from the images that although both hydrogels have cracks in the surface (fig. 13), the conductive hydrogels are more prone to cracking than

the non-conductive hydrogels which coincide with data found from rheology. Although SEM is representative of the lyphophilised gels in its dry state, alternative techniques such as CyroSEM would need to adopted to observe morphology in its hydrated state.

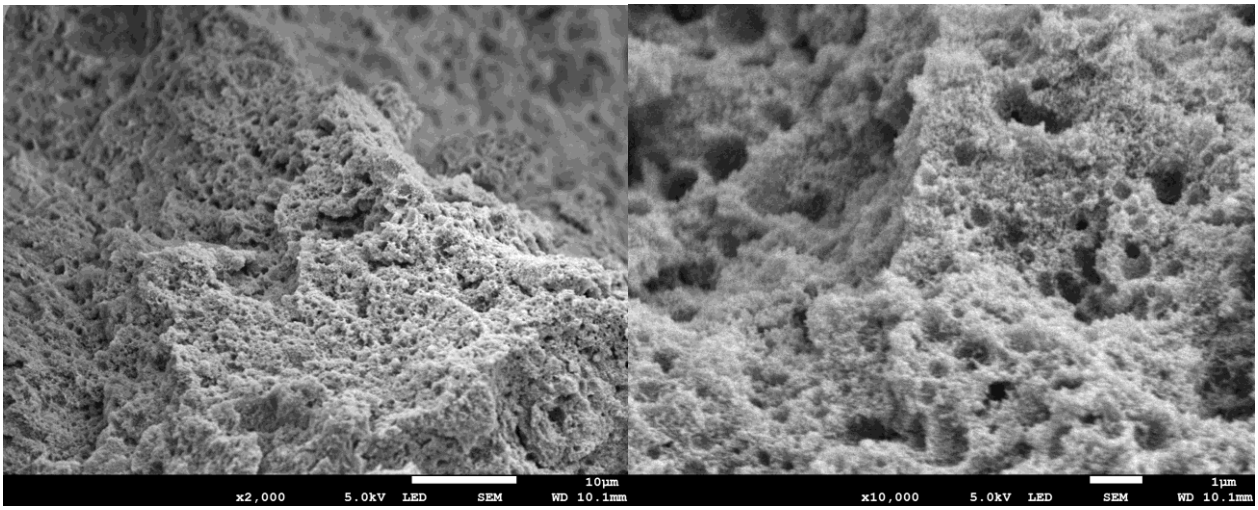

Figure 12. SEM images x2,000 and x10,000 magnification of conductive hydrogels cross sectional area.

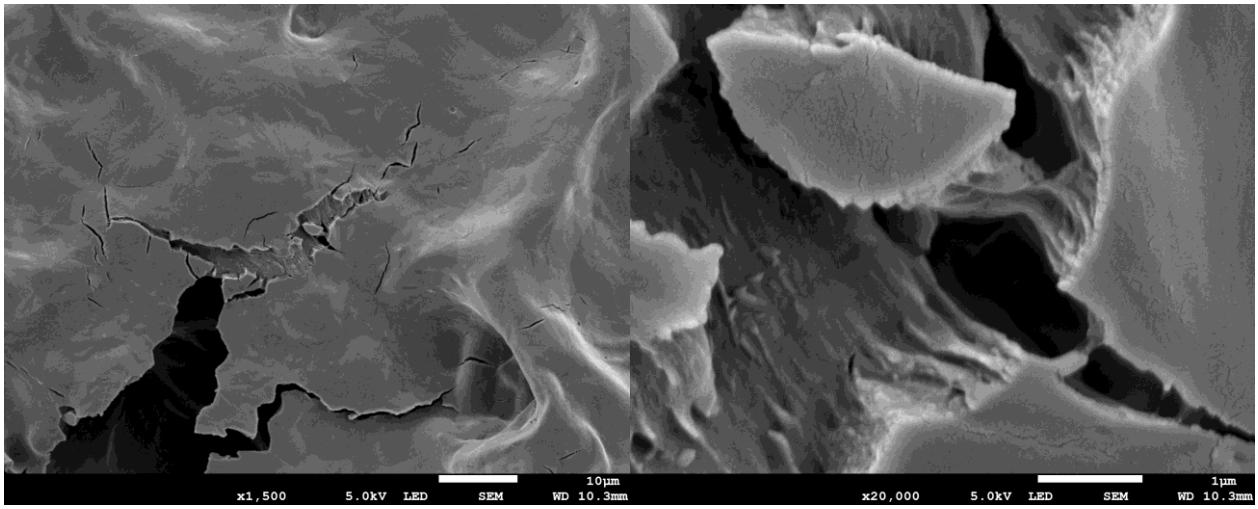

Figure 13. Morphology images from SEM x1,500 and x20,000 magnification of non-conductive cracks in hydrogel surface.

Drug Delivery Studies. After doping conductive hydrogels with PEM dissolved in water, four gels were electrochemically released and another four gels were passively released, and the quantity of PEM was determined by UV spectroscopy (fig. 13).

It is evident that between 0-30 minutes, the amount of drug released is higher when electrically triggered as opposed to the unstimulated control as expected and therefore confirms that PEM can be

electrochemically released from the hydrogels. As time increases the amount of drug released overall will also increase.

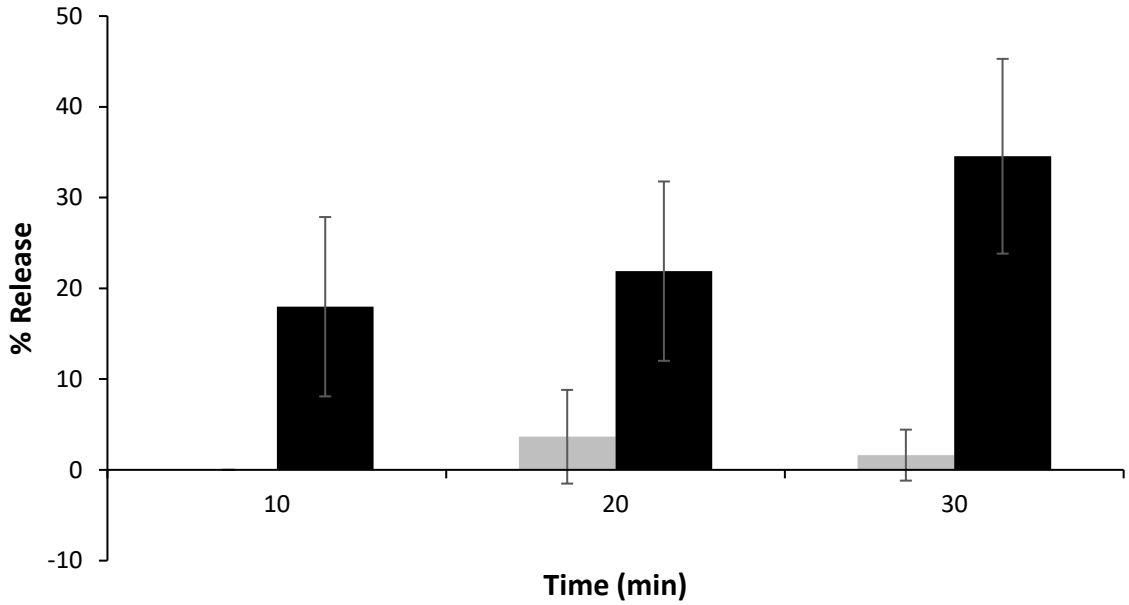

Figure 13. Drug release profiles of hydrogels loaded with PEM, without electrical stimulation (grey bars) and electrochemically triggered (black bars).

To measure the percentage of drug release, UV absorbances were recorded at 225 nm. From figure 1, absorbances were also seen from modified chitosan at 225 nm, therefore to confirm the reliability of the results obtained from drug delivery studies an additional control experiment was carried out. The same procedure was followed for the experiment above but without the presence of a drug. Briefly, the hydrogels placed on top of electrodes were electrically stimulated in deionised water as if it was PEM solution and samples were taken from electrically triggering the 'release' in PBS. When analysing the samples the absorbance of PBS at 225 nm was 0.007 and as the rest of the samples came lower than this, it can be assumed that the absorbances recorded for the samples loaded with the drug came from PEM itself.

Conclusions

Chitosan-based hydrogels were synthesized in this research displaying electrically conductive qualities that could be utilized in drug delivery. A simple methodology was used to prepare and characterize the materials using a variety of techniques (including FTIR, NMR and UV-Vis). The gels were handleable (with care), and the majority of the components of the gel were degradable (chitosan and PEGs), however the PPY is non-degradable. Future iterations of such materials will require the generation of either degradable conducting polymers or water soluble versions.

References

1 O. Michalak, M. Łaszcz, K. Jatczak, A. Witkowska, I. Bujak, A. Groman and M. Cybulski, *Molecules*, 2015, **20**, 13814–13829.

2 T. M. Allen and P. R. Cullis, *Science*, 2004, **303**, 1818–22.

3 A. T. Florence and G. W. Halbert, *Phys. Technol*, 1985, **16**, 164–176.

4 M. B. Mellott, K. Searcy and M. V Pishko, 2001, **22**, 929–941.

5 S. Feiten, R. Weide, V. Friesenhahn, J. Heymanns, K. Kleboth, H. Köppler, C. van Roye and J. Thomalla, *Springerplus*, , DOI:10.1186/s40064-016-1851-z.

6 J. Qu, X. Zhao, P. X. Ma and B. Guo, *Acta Biomater.*, 2018, 1–15.

7 L. F. Santos, I. J. Correia, A. S. Silva and J. F. Mano, *Eur. J. Pharm. Sci.*, 2018, **118**, 49–66.

8 G. Jeon, S. Y. Yang and J. K. Kim, *J. Mater. Chem.*, 2012, **22**, 14814–14834.

9 A. Banerjee, J. Qi, R. Gogoi, J. Wong and S. Mitragotri, *J. Control. Release*, 2016, **238**, 176–185.

10 Y. Zhao, Y. Wang, F. Ran, Y. Cui, C. Liu, Q. Zhao, Y. Gao, D. Wang and S. Wang, *Sci. Rep.*, , DOI:10.1038/s41598-017-03834-2.

11 S. Murdan, *J. Control. Release*, 2003, **92**, 1–17.

12 M. L. Oyen, *Int. Mater. Rev.*, 2014, **59**, 44–59.

13 Q. Chai, Y. Jiao and X. Yu, *Gels*, 2017, **3**, 6.

14 N. A. Peppas, P. Bures, W. Leobandung and H. Ichikawa, *Eur. J. Pharm. Biopharm.*, 2000, **50**, 27–46.

15 J. G. Hardy, J. Y. Lee and C. E. Schmidt, *Curr. Opin. Biotechnol.*, 2013, 24, 847–854.

16 K. T. Nguyen and J. L. West, *Biomaterials*, 2002, **23**, 4307–4314.

17 K. Y. Lee and D. J. Mooney, *Chem. Rev.*, 2001, **101**, 1869–1879.

18 R. A. Horch, N. Shahid, A. S. Mistry, M. D. Timmer, A. G. Mikos and A. R. Barron, *Biomacromolecules*, 2004, **5**, 1990–1998.

19 C. S. Linsley and B. M. Wu, *Ther. Deliv.*, 2017, **8**, 89–107.

20 Z. Li, H. Shim, M. O. Cho, I. S. Cho, J. H. Lee, S.-W. Kang, B. Kwon and K. M. Huh, *Carbohydr. Polym.*, 2018, **184**, 342–353.

21 M. Kashi, F. Baghbani, F. Moztarzadeh, H. Mobasheri and E. Kowsari, *Int. J. Biol. Macromol.*, 2018, **107**, 1567–1575.

22 K. Wang, Q. Fu, X. Chen, Y. Gao and K. Dong, *RSC Adv.*, 2012, **2**, 7772–7780.

23 L. Li, J. Ge, B. Guo and P. X. Ma, *Polym. Chem.*, 2014, **5**, 2880.

24 N. S. Walia, B. S. Rathore and A. K. Jaiswal, *Med. journal, Armed Forces India*, 2000, **56**, 27–28.

25 T. Batista Napotnik and D. Miklavčič, *Bioelectrochemistry*, 2018, 120, 166–182.

26 J. Shang, Z. Shao and X. Chen, *Polymer (Guildf).*, 2008, **49**, 5520–5525.

27 D. S. Wallace, A. J. Fisher, W. Hayes, A. M. Stoneham and A. Testa, *J. Phys.: Condens. Matter*, 1991, **3**, 3905-3920.

28 B. Guo, L. Glavas and A. C. Albertsson, *Prog. Polym. Sci.*, 2013, **38**, 1263–1286.

29 J. G. Hardy, D. J. Mouser, N. Arroyo-Currás, S. Geissler, J. K. Chow, L. Nguy, J. M. Kim and C. E. Schmidt, *J. Mater. Chem. B*, 2014, **2**, 6809–6822.

30 L. Hu, Y. Sun and Y. Wu, *Nanoscale*, 2013, **5**, 3103.

31 B. Guo, A. Finne-Wistrand and A. C. Albertsson, *Biomacromolecules*, 2011, **12**, 2601–2609.

32 M. N. V. R. Kumar, R. A. A. Muzzarelli, C. Muzzarelli, H. Sashiwa and A. J. Domb, *Chem. Rev.*, 2004, **104**, 6017–6084.
33 R. C. F. Cheung, T. B. Ng, J. H. Wong and W. Y. Chan, *Mar. Drugs*, 2015, 13, 5156–5186.
34 A. Anitha, S. Sowmya, P. T. S. Kumar, S. Deepthi, K. P. Chennazhi, H. Ehrlich, M. Tsurkan and R. Jayakumar, *Prog. Polym. Sci.*, 2014, **39**, 1644–1667.
35 R. Jayakumar, D. Menon, K. Manzoor, S. V Nair and H. Tamura, *Carbohydr. Polym.*, 2010, 82, 227–232.
36 S. Rodrigues, M. Dionísio, C. Remuñán López and A. Grenha, *J. Funct. Biomater*, 2012, **3**, 615–641.
37 P. Sorlier, A. Denuzire, C. Viton, A. Domard and A. Denuzie, *Society*, 2001, **2**, 765–772.
38 S. Luo, J. Cao and A. G. McDonald, *Ind. Crops Prod.*, 2018, **121**, 169–179.
39 V. E. Yudin, I. P. Dobrovolskaya, I. M. Neelov, E. N. Dresvyanina, P. V Popryadukhin, E. M. Ivan'kova, V. Y. Elokhovskii, I. A. Kasatkin, B. M. Okrugin and P. Morganti, *Carbohydr. Polym.*, 2014, **108**, 176–182.
40 K. Wang, L. S. Loo and K. L. Goh, *Mater. Res. Express*, 2016, **3**, 0.
41 Y. Liu, X. Peng, H. Ye, J. Xu and F. Chen, *Polym. - Plast. Technol. Eng.*, 2015, **54**, 411–415.
42 X. Zhang, D. Yang and J. Nie, *Int. J. Biol. Macromol.*, 2008, **43**, 456–462.
43 P. Kolhe and R. M. Kannan, *Biomacromolecules*, 2003, **4**, 173–180.
44 B. D. Ulery, L. S. Nair and C. T. Laurencin, *J. Polym. Sci. Part B Polym. Phys.*, 2011, 49, 832–864.
45 M. B. Browning and E. Cosgriff-Hernandez, *Biomacromolecules*, 2012, **13**, 779–786.
46 N. K. E. Guimard, J. L. Sessler and C. E. Schmidt, *Macromolecules*, 2009, **42**, 502–511.
47 J. Kumirska, M. Czerwicka, Z. Kaczyński, A. Bychowska, K. Brzozowski, J. Thöming and P. Stepnowski, *Mar. Drugs*, 2010, 8, 1567–1636.
48 G. Ma, X. Zhang, J. Han, G. Song and J. Nie, *Int. J. Biol. Macromol.*, 2009, **45**, 499–503.
49 Q. Li, D. Yang, G. Ma, Q. Xu, X. Chen, F. Lu and J. Nie, *Int. J. Biol. Macromol.*, 2009, **44**, 121–127.
50 C. Gartner, B. L. Löpez, L. Sierra, R. Graf, H. W. Spiess and M. Gaborieau, *Biomacromolecules*, 2011, **12**, 1380–1386.
51 L. Heux, J. Brugnerotto, J. Desbrières, M. F. Versali and M. Rinaudo, *Biomacromolecules*, 2000, **1**, 746–751.
52 F. Devreux, G. Bidan, A. A. Syed and C. Tsintavis, *J. Phys.*, 1985, **46**, 1595–1601.
53 M. Forsyth, V.-T. Truong and M. E. Smith, *Polymer (Guildf).*, 1994, **35**, 1593–1601.
54 R. M. Souto-Maior, M. I. B. Tavares and E. E. C. Monteiro, *Solid State 13 C NMR Study of Methyl Methacrylate-Methacrylic Acid Copolymers*, 2005, vol. 4.
55 P. P. Dhawade* and R. N. Jagtap, *Pelagia Res. Libr. Adv. Appl. Sci. Res.*, 2012, **3**, 1372–1382.
56 L. S. Guinesi and É. T. G. Cavalheiro, *Thermochim. Acta*, 2006, **444**, 128–133.
57 F. Ferrero and M. Periolatto, *J. Nanosci. Nanotechnol.*, 2012, **12**, 4803–4810.
58 M.-K. Song, Y.-T. Kim, Y. T. Kim, B. W. Cho, B. N. Popov and H.-W. Rhee, *J. Electrochem. Soc.*, 2003, **150**, A439.
59 D. Watkins, M. Hosur, A. Tcherbi-narteh and S. Jeelani, *Integr. Med. Res.*, 2014, **4**, 26–32.
60 C. Peniche-Covas, W. Argüelles-Monal and J. San Román, *Polym. Degrad. Stab.*, 1993, **39**, 21–28.
61 I. Corazzari, R. Nisticò, F. Turci, M. G. Faga, F. Franzoso, S. Tabasso and G. Magnacca, *Polym.*

Degrad. Stab., 2015, **112**, 1–9.

62 K. Hyun, M. Wilhelm, C. O. Klein, K. S. Cho, J. G. Nam, K. H. Ahn, S. J. Lee, R. H. Ewoldt and G. H. McKinley, *Prog. Polym. Sci.*, 2011, **36**, 1697–1753.

63 B. Guo, A. Finne-Wistrand and A. C. Albertsson, *Chem. Mater.*, 2011, **23**, 1254–1262.

64 X. Ji, Z. Zhang, J. Chen, G. Yang, H. Chen and L. A. Lucia, *BioResources*, 2017, **12**, 5395–5406.

Chapter 2: Injectable electroactive hydrogels

Abstract

Hydrogels were synthesised via Schiff bases between self-crosslinking chitosan and oxidised hyaluronic acid. Successful synthesis was confirmed with FTIR and NMR, and characterisation of the gels included DSC, TGA and XRD.

Introduction

There is a market need for biomaterials capable of well controlled drug delivery. Systems can be designed to enable controlled and localized drug delivery to optimise the therapeutic effect of the drug (and hopefully minimize side effects).[1] Patient compliance should improve as drug concentrations will be maintained at a desired level (ideal for patients with chronic illnesses).[2] Commercially available systems (e.g. drug pump) tend to be inflexible and rate of drug release is already determined. By using stimuli responsive drug delivery systems, there may be more control over the concentration of drug released after administration of the delivery system hence can be tailored to each person's needs. Although externally responsive drug delivery systems were first reported in the late 1970s,[3] there are various types of external stimuli still currently being explored such as light,[4] pH,[5,6] temperature,[7] electricity,[8] enzymes[9] and magnetic fields[10]. They can take the forms of hydrogels, lipids, nanoparticles and polymeric micelles.[11] Hydrogels are promising materials for biomedical purposes, namely drug delivery, tissue engineering and biosensors, due to their swelling ability to absorb large amounts of water so that they closely resembles biological tissues (this also contributes to gels biocompatibility and mechanical properties).[12] Their porous structure is formed from a network of physical or chemical crosslinking between polymer chains, and this highly solvated matrix can hold and protect drugs from harsh environments.[13] Another appealing property of hydrogels is that they can be synthesised with enzyme degradable links (e.g. amide or ester bonds) rendering them biodegradable or they may be chemically stable. Biodegradable systems are typically designed for short term applications (e.g. as drug delivery systems or tissue scaffolds for tissue engineering).

While each type of stimuli has its own advantages, the use of electrical triggers has the benefits of switchable ON-OFF release, the magnitude of current can be controlled precisely and duration and intervals does not have to be predetermined.[14] Conducting polymers (CPs) have electrical properties close to semiconductors/metals. They are easy to synthesise either via electrochemical means or by chemical oxidation. They were invented in 1977 and the first conductive polymer discovered was polyacetylene by Shirakawa et al.[15,16] This led to extensive exploration in CPs and their applicability to a wide range of fields such as biomedical applications for example drug delivery[17] and, also in modern day technology for instance organic light-emitting diodes[18]. Other CPs include poly-(3,4-ethylenedioxythiophene) (PEDOT), polypyrrole and polyaniline. Drug carriers with the inclusion of CPs have received considerable amounts of attention a decade after its discovery due to their compatibility with biological tissues and potential for ON-OFF release profiles.[19] In addition to the facile synthesis of the CP, the drug can be incorporated of the with ease. Pharmaceutical compounds can be dissolved in a solvent and electrochemically loaded or they may be encapsulated in the polymer during polymerisation. The mechanism behind switchable release relies on the doped polymer changing from its oxidised state to its redox state. The transition from one state to the other involves diffusion of hydrated ions within the polymer.[20] Not only are drugs possible to be loaded, it is possible for molecules

like neurotransmitters[21] as well as growth factors[22]. Because of the chemistry of CPs, it is feasible to include various functionalities in order to get desirable traits from the material. Electroactive hydrogels can be designed with ester or amide moieties making them biodegradable by biological enzymes (e.g. esterase).

Natural polymers are widely accepted to be more compatible with biological molecules and it is typical for hydrogels to be a blend of synthetic and naturally occurring polymers as this enables their properties to be tuned with ease. Being FDA (Food and Drug Administration) approved already, chitosan has received great attention in biomedicine because of its low toxicity in vivo (cite) and biocompatibility. It is a positively charge polysaccharide and can be produced from the deacetylation of chitin found in the shells of crustaceans. Along its backbone contains amine units which allow for easy manipulation to adjust its chemical properties for example, enhancing the solubility. Hyaluronic acid (HA) is also FDA approved and an anionic polymer that is present in tissues throughout the body (e.g. epithelial and neural tissues), hence research on incorporating hyaluronic acid in biomaterials has grown exponentially in the past few years.[23] HA hydrogels require crosslinking which necessitates chemical modifcation to ensure stability.[24]

The aim of this study is to start the process of producing injectable hydrogels combining two naturally occurring polymers that are inherently biocompatible for biomedical applications, namely drug delivery. By introducing PEDOT into the network, we hope to successfully synthesise an electroactive hydrogel capable of controlled drug delivery.

Experimental

Materials

All reagents were used as received without further purification and purchased from Sigma-Aldrich or Thermo Fisher.

Synthesis

Oxidising hyaluronic acid to display aldehydes (HA-ALD). Sodium hyaluronate (1 g) and sodium periodate (0.535 g, 2.5 mmol) was dissolved in ultrapure water (100 mL) and left to stir for 24 hours at room temperature in the dark. After oxidising, ethylene glycol (140 μL, 2.5 mmol) was added to eliminate unreacted periodate and stirred for a further hour in the dark. The mixture was then transferred into cellulose dialysis tubing membranes (MWCO 3500) and the product was dialyzed against 2 litres of ultrapure (milli Q) water in order to remove low molecular weight contaminants. The water every 2 hours during the day for 4 days after which it was lyphophilised.

Chitosan stock solution. Medium molecular weight chitosan (2 g) was added to 1% acetic acid and water (100 mL) and stirred until complete dissolution. The pH was adjusted to around 5.5 by addition of sodium hydroxide (~14 mL, 1 M) and agitated for 24 hours.

Aminoxy-terminated EDOT (EDOT-OHN_2). Synthesis of phthalimide-terminated EDOT: triphenylphosphine (1.71 g) and N-hydroxyphthalimide (1.06 g) was stirred with hydroxymethyl EDOT (1.15 g) in dichloromethane (50 mL). Diisopropyl azodicarboxylate (1.128 g, 1.128 mL) (density = 1.027 g/cm^3) was added to the solution and left stirring for 24 hrs. After, the solution was dried on the rotary evaporator. The sample was then dissolved in dichloromethane and compounds were separated through column chromatography following TLC analysis. Solutions containing product and impurities were purified again by chromatography and dried.

Cleavage of phthalimide moieties: precipitate obtained was added to hydrazine hydrate (10 mL) and left under nitrogen for 24 hours. Solution was then stirred for 2 hours before performing TLC. Afterwards, solution was distilled through rotary evaporator at 50°C, 13 mBar. Purification via column chromatography was performed on the resulting mixture.

Sulfonate-terminated EDOT (EDOT-S). Hydroxymethyl EDOT (0.8 g), sodium hydride (0.1228 g) and toluene (12.5 mL) was refluxed under nitrogen at 90°C for 2 hrs. Butane sultone (0.476 mL) was placed into the flask and continued to reflux for a further 2 hrs. When reaction mixture was cool, product was precipitated with acetone and dried under high vacuum.

Polymerisation of aminoxy-terminated EDOT and sulfonate-terminated EDOT. Mixtures of EDOT-S and EDOT-OHN_2 was prepared at four different molar ratios:

Molar ratios		
	EDOT-S	**EDOT-ONH_2**
A	1	1
B	5	1
C	10	1

EDOT-ONH_2 was dissolved in a combination of ethanol and distilled water and 0.4 mL was placed into plastic falcons labelled A, B and C corresponding to each molar ratio containing pre-weighed EDOT-S. Each container was manually stirred with water (5 mL) to dissolve EDOT-S.

Ammonium persulfate (2 q) was added into each solution. Subsequently oxidative polymerisation occurred using iron chloride (5 mg) and purified via dialysis. Resulting products were freeze-dried.

Hydrogel preparation. Solutions of HA-ALD (0.25 wt% in PBS) and CS (2 wt%) were prepared. In this research four different hydrogel formulations were fabricated, non-conductive chitosan-HAALD (CS-HAALD), PEDOT A-CA-HAALD, PEDOT B-CS/HAALD, PEDOT C/HA-ALD. The yield for molar ratio D was not enough for characterisation. Each PEDOT derivative was dissolved 2.5 wt% PEDOT-A was dissolved in water, B – water and C – PBS.

Hydrogels were prepared at room temperature, oxidised hyaluronic acid (HA-ALD) was added to chitosan solution in the ratio of 1:2. For conductive hydrogels, the ratio was also 1:2 PEDOT to chitosan and was mixed with chitosan before the addition of oxidised hyaluronic acid. For clarity, throughout this report hydrogels of chitosan crosslinked with HA-ALD will be defined as non-conductive and ones containing PEDOT A, B and C will be noted A, B and C respectively. The solutions of EDOT-S and EDOT-ONH_2 will be referred to as PEDOT A, B and C.

Characterisation

Fourier Transform Infrared – attenuated total reflectance mode (FTIR-ATR). Spectra were recorded with an Agilent Technologies Infrared Spectrometer in ATR mode with the range 500-4000 cm^{-1}. All data was baseline corrected in ResPro.

Solution state NMR. Bruker AVANCE III 400 (NanoBay) with a 5 mm ^{1}H-X broadband observe (BBO, 109Ag-19F) RT probe was used to record proton NMR spectra.

Sample preparation for chitosan (MMW), 1 mg/mL was dissolved in 2% DCl (35 wt% in D_2O)/D_2O, hyaluronic acid was dissolved in D_2O, 5 mg/mL and modified HA 5mg/mL was stirred in D_2O for ca. 2 hours. For reference ((3-Trimethylsilyl)propanoic-2,2,3,3-d_4) was dissolved in all samples.

Differential Scanning Calorimetry (DSC). DSC experiments were carried out using a Mettler Toledo DSC1 SOP. The pans used for measurements were 40 μL.

Thermogravimetric analysis (TGA). Thermal stability of samples were investigated using a NETZSCH STA 449 F3 Jupiter thermal analyser with alumina reference pan from temperature ranges 25 to 550°C.

X-ray diffraction (XRD). Diffractograms were observed using a Rigaku SmartLab powder diffractometer in a 2θ from 5 to 40° and a resolution of 0.1°.

Results and Discussion

Synthesis. Sodium periodate is well known for selective oxidation of diol groups and was therefore used to oxidise hyaluronic acid forming two aldehyde groups. The aldehydes will then react with the primary amine groups attached to chitosan in principle forming a Schiff base (Scheme 1) linkage which crosslinks the hydrogel. When stirring the mixture, after a short period of time the mixture gelated (Image 1). Although gelation is evident, they would not be able to hold their shape if taken out of Eppendorf tubes.

However this reaction is reversible, and thus terminating PEDOT with aminoxy groups creates an irreversible reaction whilst also providing conductivity in the gels. Another common problem for conducting polymers is the solubility (which tends to be poor). This was counteracted by modifying PEDOT with sulfonate rendering it soluble in either in water or PBS.

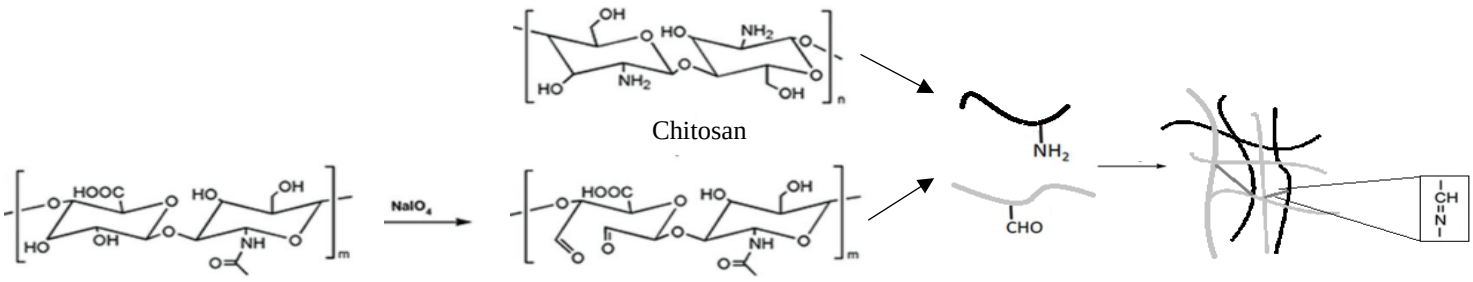

Scheme 1. Formation of Schiff bases between chitosan and oxidised hyaluronic acid.

Image 1. Visual representation of hydrogels before (left) and after (right) crosslinking with PEDOT C.

FTIR-ATR mode. To compare the difference in spectra, hyaluronic acid is overlapped with oxidised hyaluronic acid in Figure 1. Both spectra are very similar, as the only difference between the two chemical structures are the addition of two aldehyde moieties. Influences from carboxylic acid (O-H stretch) can be assigned to the broad band dominating between 3000-3670 cm^{-1}. C=O bonds are related to the peak at 1600 cm^{-1}. The most significant peak to indicate successful synthesis of HA-ALD from HA is a peak attributed to vibrations from H-C=O. On the spectra of HA-ALD this peak arises at 1718 cm^{-1} and therefore confirms HA modification.

FTIR spectra of chitosan medium molecular weight (CS) with 75-85% deacetylation is shown in Figure 2. At around 3350 cm^{-1} there is broad absorbance correlating to -OH stretch in alcohols which is also present in both hyaluronic acid (HA) and oxidised hyaluronic acid (HA-ALD). Typically an absorbance from $-NH_2$ stretching would be expected in the same range as -OH at ~3400 and 3500 cm^{-1} however because of the broadness of the -OH peak, the signal has been overlapped. Aromatic overtones (C-H stretch) would also be hidden at ~3010 cm^{-1}. Other evidence to suggest the presence of amine groups can be confirmed by the peak at 1566 cm^{-1} which can be linked to an N-H bend. Ether C-O-C stretches are shown at ~1150 cm^{-1} from the polymer structure. C-O stretches present could be responsible for sharp peaks occurring at 1020 and 1057 cm^{-1}. It is also likely to see amide I and II around 1600 and 1550 cm^{-1}, respectively for the reason that chitosan is partially deacetylated.

IR spectra of HA-ALD and non-conductive hydrogels are given in Figure 2. A new peak at 1618 cm^{-1} appears from C=N group along with the absence at 1587 and 1718 cm^{-1} from N-H bending and aldehyde confirms the structure of a Schiff base formation.

The FTIR spectra of PEDOT can be found in previous literature. Selvagnesh et al. reported stretching modes of C=C and C-C at 1518, 1483 and 1339 cm^{-1} due to the thiophene ring.[25] Absorptions at ~930 and 691 cm^{-1} are vibrations from C-S in the thiophene ring and around 1093-1076 and 1052-1047 cm^{-1} are attributed to ethylene dioxy group.[26] In the spectra of PEDOT A obtained (fig. 3, grey solid curve), C=C and C-C vibrations absorbances at 1636 and 1455 cm^{-1} represent each bond respectively. The peak at 730 cm^{-1} could come from vibrations of C-S bond. The peaks occurring around 1330 cm^{-1} correspond to S=O stretching of the sulfonate bonds.

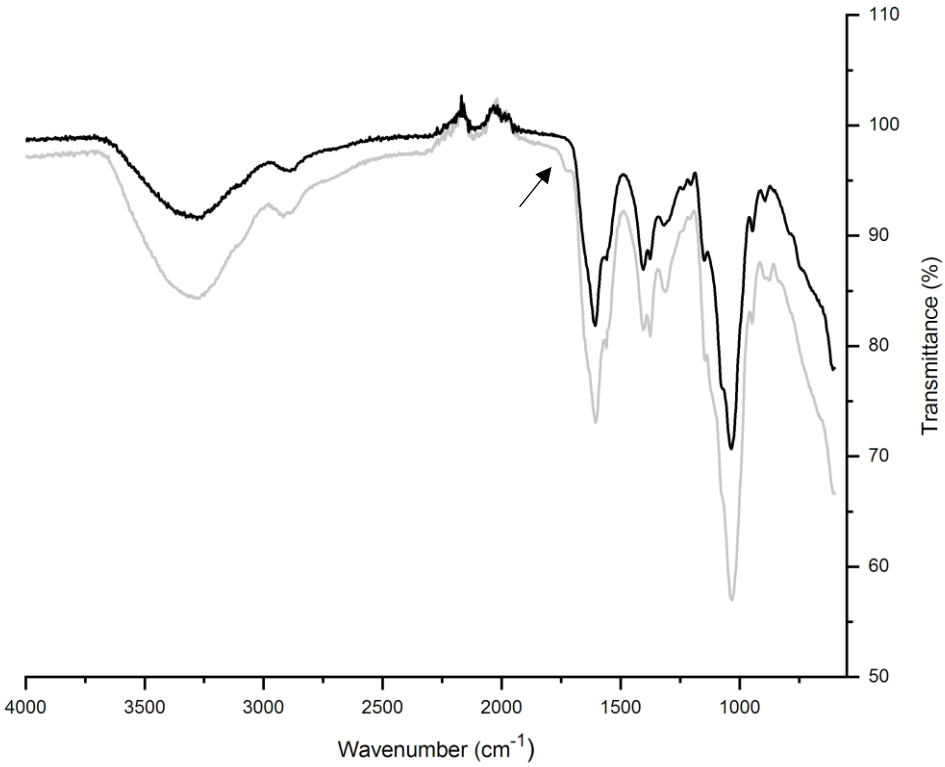

Figure 1. FTIR of hyaluronic acid (black) and oxidised hyaluronic acid (grey).

Figure 2. FTIR of chitosan (black), oxidised hyaluronic acid (dashed black) and non-conductive hydrogel (grey).

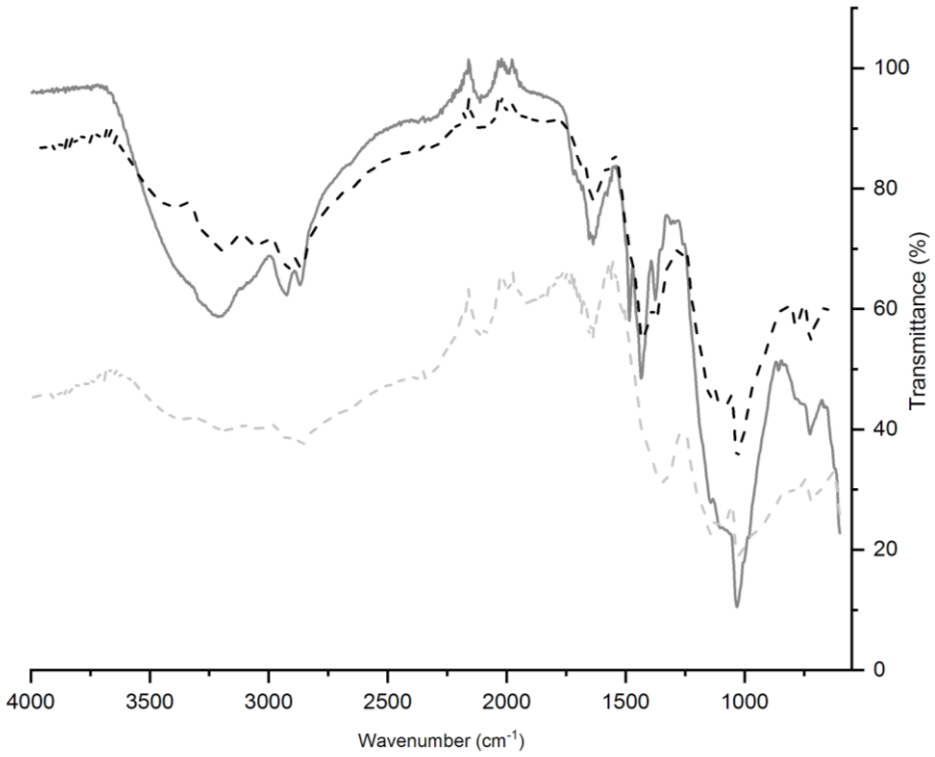

Figure 3. FTIR spectra of PEDOT A, (grey solid); PEDOT B, (black dashed) and PEDOT C, (grey dashed).

Solution state ^{1}H NMR. Proton NMR spectra of chitosan is shown in Figure 4. The HOD solvent peak is found around 4.79 ppm. From this spectra, the degree of deacetylation can be calculated by assigning the resonance between 3 and 4 ppm to H2-H6 of the ring and integrating the peaks to 6000 representing 6 protons. This results in an integration value of 73.47 to the peak at 2.03 ppm which is assigned to -CH_3 of the alkylated GlcN unit and therefore the degree of deacetylation will be approximately 88%.

$$\frac{74}{600} \times 100 = \sim 12\ \%$$

Specifically, H2 is responsible for the singlet at 3.10 ppm and the multiplet ~3.5 to 4 ppm are assigned to H3-H6.

Hyaluronic acid (Fig. 5) and chitosan both contain GlcNAc monomers and therefore the broad multiplet in the same region between 3-4 ppm can also be said to be hydrogens in the sugar ring where, likewise, the peak at 3.3 corresponds to the proton attached to GlNAc. Anomeric protons would also produce a signal at 4.8 ppm however due to a sharp signal from D_2O solvent (doublet) has overlapped.[27]

In contrast, oxidised hyaluronic acid (Fig. 5) produces new chemical shifts at 4.9, 5.1 and 5.2 ppm establishing the presence of aldehyde groups which are in agreement with previous literature, confirming successful synthesis.[28] The degree of oxidation of hyaluronic acid was ~30.4 % and was quantified by comparing the integrals of the aldehyde and acetamide (2.04 ppm).

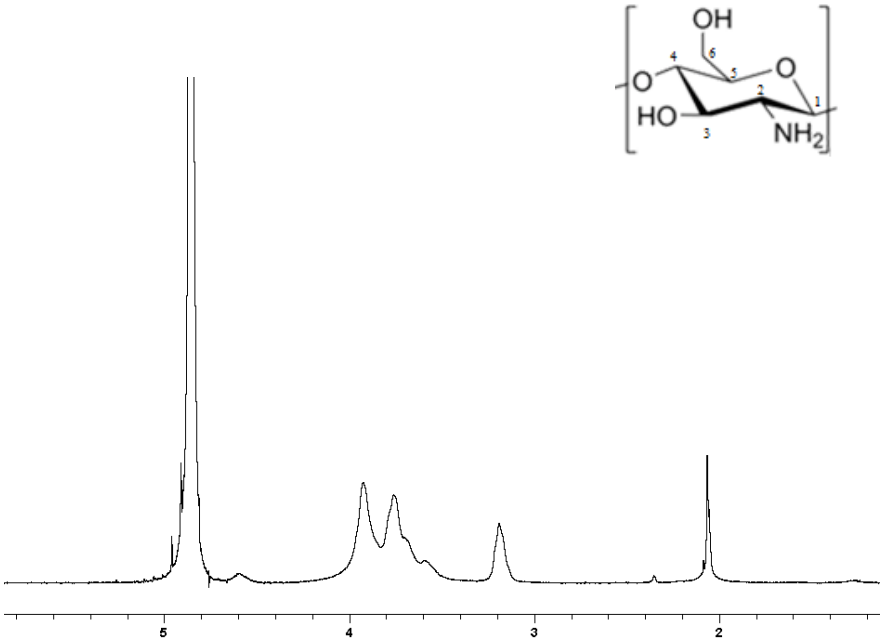

Figure 4. ^{1}H NMR spectra of chitosan.

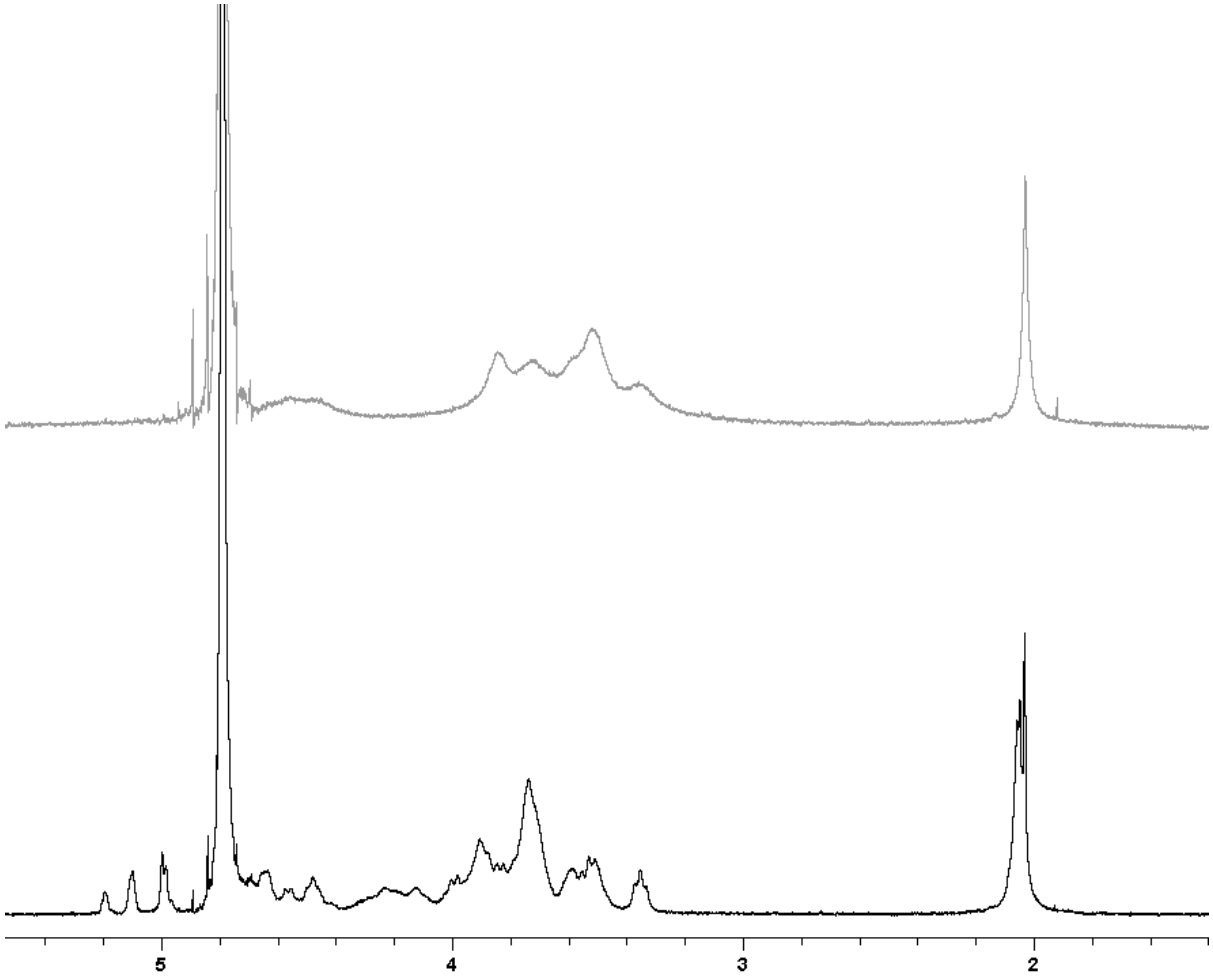

Figure 5. ^{1}H NMR spectra of hyaluronic acid (grey) and oxidised hyaluronic acid (black).

Differential scanning calorimetry. DSC was run on the four hydrogel formulations: non-conductive, A, B and C displayed in figure 6. The samples were heated from -20 to 200°C. The curves for chitosan and hyaluronic acid can be found in the literature. Characteristic temperatures of chitosan are typically found around 110-117 and 295°C where the lower temperature is found to be its glass transition temperature and the higher temperature is because of the decomposition of amine units.[29] Hyaluronic acid displays a singular exothermic peak at 240°C because of its degradation.[30] After crosslinking, figure 6 (black solid) exhibits a peak at 114°C and 295°C peak from chitosan cannot be seen proving evidence of the polymerisation between the two components.

Hydrogel A, B and C all showed one peak at 105, 138 and 146°C accordingly signifying that as the amount of EDOT-S increases the thermal stability of the hydrogels will also increase. It is noticeable that none of the hydrogels show a definite glass transition state.

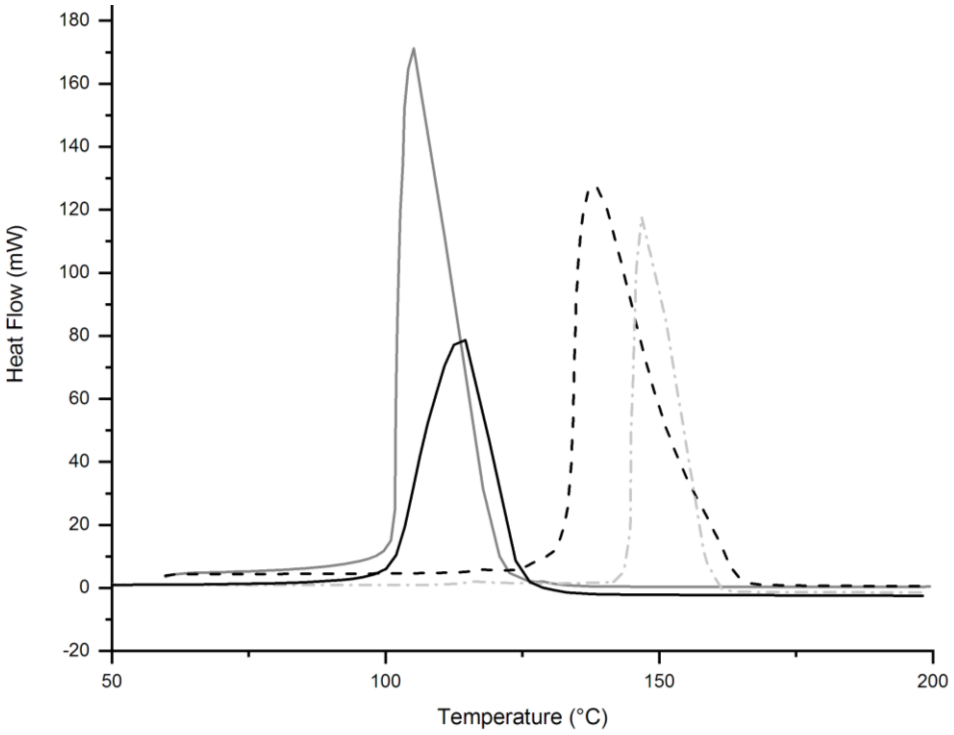

Figure 6. DSC thermograms of hydrogels: non-conductive (black solid), A (grey solid), B (black dashed) and C (grey dashed).

Thermogravimetric analysis. TGA thermograms for the hydrogels are shown in Figure 7. From 50°C to approximately 150°C all gels show major weight loss due to evaporation of water. The peaks at ca. 240°C corresponds to the mass loss upon degradation of the polymers.

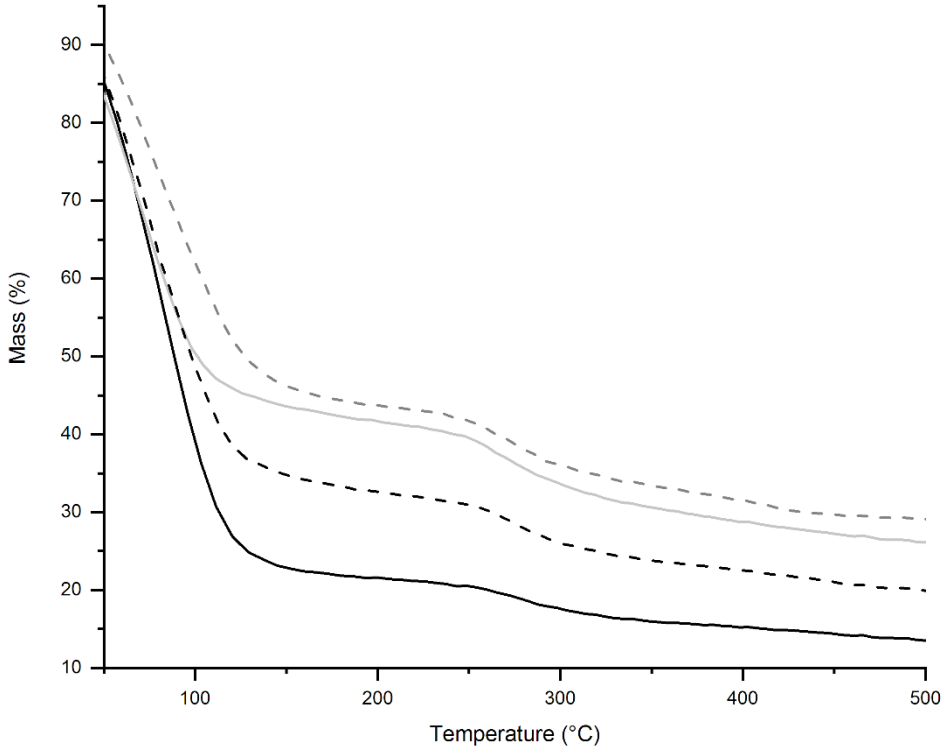

Figure 7. TGA thermograms of hydrogels: non-conductive (black solid), A (grey solid), B (black dashed) and C (grey dashed).

X-ray diffraction. Hydrogels containing PEDOT showed the same XRD pattern and so, they are represented with one curve. Figure 8 shows the XRD analysis of both the non-conductive hydrogels and conductive hydrogels containing the PEDOT derivatives. The curve from non-conductive hydrogel peaks at 2θ = 27.9°. Both polysaccharides are semi-crystalline with characteristic peaks at 10.3, 15.9 and 20.1° for CS and at 28, 47 and 56° for HA.[27,31] The broad peaks appear to show that the polysaccharides are not well organised (i.e. non-crystalline) and they are amorphous in the hydrogel.

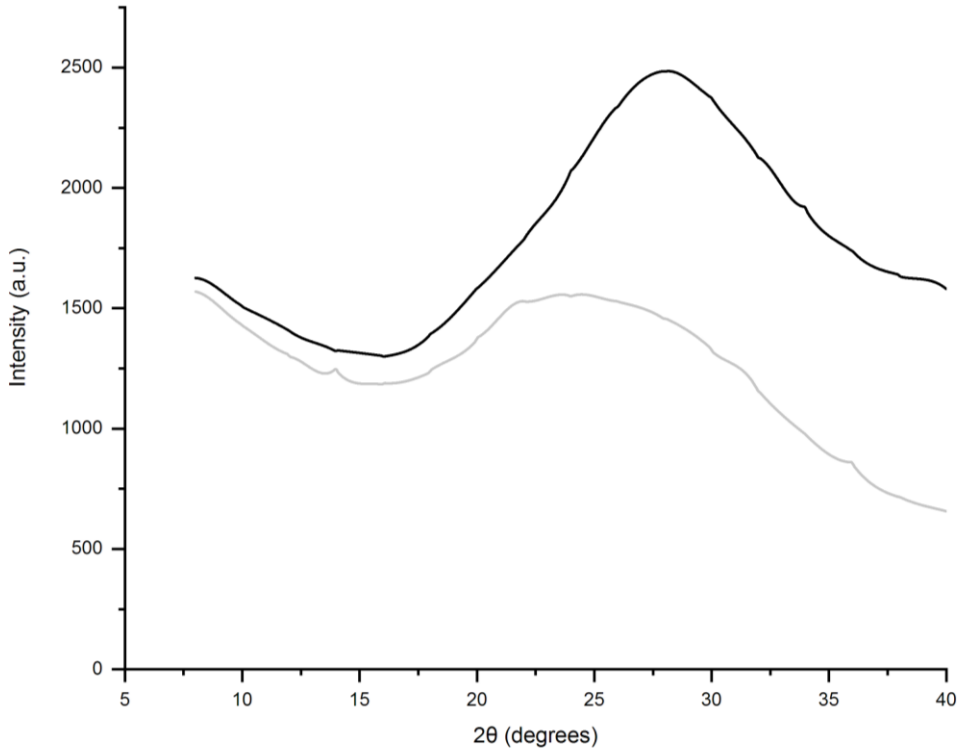

Figure 8. XRD pattern of non-conductive hydrogel (black) and conductive hydrogel (grey).

Conclusions

In this research a method to produce self-crosslinking hydrogels was proposed. Different analytical techniques (FTIR and NMR) were used to confirm successful gel formation between chitosan and oxidised hyaluronic acid which resulted in gel formation. The thermal properties and XRD patterns of the gels were investigated to characterise its thermal stability and degree of crystallinity. Further development of these hydrogels is necessary and future experiments must focus on the generation of robust gels and their electrochemical properties (i.e. its conductivity) for electrochemically triggered drug delivery.

References

1 G. Jeon, S. Y. Yang and J. K. Kim, *J. Mater. Chem.*, 2012, **22**, 14814–14834.

2 D. Svirskis, J. Travas-Sejdic, A. Rodgers and S. Garg, *J. Control. Release*, 2010, **146**, 6–15.

3 D. Liu, F. Yang, F. Xiong and N. Gu, *Theranostics*, 2016, 6, 1306–1323.

4 Y. Yao, X. Chi, Y. Zhou and F. Huang, *Chem. Sci.*, 2014, **5**, 2778–2782.

5 J. Qu, X. Zhao, P. X. Ma and B. Guo, *Acta Biomater.*, 2017, **58**, 168–180.

6 S. Nitta, S. Kaketani and H. Iwamoto, *Eur. Polym. J.*, 2015, **67**, 50–56.

7 X. Gu, J. Wang, X. Liu, D. Zhao, Y. Wang, H. Gao and G. Wu, *Soft Matter*, 2013, **9**, 7267–7273.

8 M. Kashi, F. Baghbani, F. Moztarzadeh, H. Mobasheri and E. Kowsari, *Int. J. Biol. Macromol.*, 2018, **107**, 1567–1575.

9 A. A. Aimetti, A. J. Machen and K. S. Anseth, *Biomaterials*, 2009, **30**, 6048–6054.

10 Q. Zhang, J. Liu, K. Yuan, Z. Zhang, X. Zhang and X. Fang, *Nanotechnology*, 2017, **28**, 405101.

11 J. Qu, X. Zhao, P. X. Ma and B. Guo, *Acta Biomater.*, 2018, 1–15.

12 N. Sood, A. Bhardwaj, S. Mehta and A. Mehta, *Drug Deliv.*, 2016, 23, 758–780.

13 Q. Chai, Y. Jiao and X. Yu, *Gels*, 2017, **3**, 6.

14 S. Murdan, *J. Control. Release*, 2003, **92**, 1–17.

15 H. Shirakawa, E. J. Louis, A. G. MacDiarmid, C. K. Chiang and A. J. Heeger, *J. Chem. Soc. Chem. Commun.*, 1977, **36**, 578–580.

16 S. C. Rasmussen, *Bull. Hist. Chem.*, 2014, **39**, 64–72.

17 S. Mongkolkitikul, N. Paradee and A. Sirivat, *Eur. J. Pharm. Sci.*, 2018, **112**, 20–27.

18 J. W. Huh, Y. M. Kim, Y. W. Park, J. H. Choi, J. W. Lee, J. W. Lee, J. W. Yang, S. H. Ju, K. K. Paek and B. K. Ju, *J. Appl. Phys.*, 2008, **103**, 44502.

19 B. Guo, L. Glavas and A. C. Albertsson, *Prog. Polym. Sci.*, 2013, **38**, 1263–1286.

20 X. Luo and X. T. Cui, *Electrochem. commun.*, 2009, **11**, 402–404.

21 R. Wadhwa, C. F. Lagenaur and X. T. Cui, *J. Control. Release*, 2006, **110**, 531–541.

22 B. C. Thompson, S. E. Moulton, J. Ding, R. Richardson, A. Cameron, S. O'Leary, G. G. Wallace and G. M. Clark, *J. Control. Release*, 2006, **116**, 285–294.

23 D. Bermejo-Velasco, W. Dou, A. Heerschap, D. Ossipov and J. Hilborn, *Carbohydr. Polym.*, 2018, **197**, 641–648.

24 F. Dosio, S. Arpicco, B. Stella and E. Fattal, *Adv. Drug Deliv. Rev.*, 2015, **97**, 204–236.

25 S. V. Selvaganesh, J. Mathiyarasu, K. L. N. Phani and V. Yegnaraman, *Nanoscale Res. Lett.*, 2007, **2**, 546–549.

26 P. Damlin, C. Kvarnström and A. Ivaska, *J. Electroanal. Chem.*, 2004, **570**, 113–122.

27 M. H. Abu Elella, R. R. Mohamed and M. W. Sabaa, *Carbohydr. Polym.*, 2018, **189**, 107–114.

28 Y. Huang, X. Zhang, A. Wu and H. Xu, *RSC Adv.*, 2016, **6**, 33529–33536.

29 F. Ferrero and M. Periolatto, *J. Nanosci. Nanotechnol.*, 2012, **12**, 4803–4810.

30 E. Larrañeta, M. Henry, N. J. Irwin, J. Trotter, A. A. Perminova and R. F. Donnelly, *Carbohydr. Polym.*, 2018, **181**, 1194–1205.

31 P. P. Dhawade* and R. N. Jagtap, *Pelagia Res. Libr. Adv. Appl. Sci. Res.*, 2012, **3**, 1372–1382.

Conclusions and Future Work

Conclusions

Hydrogels were successfully synthesised by different two fundamentally different methods, potentially enabling two different methods of application to a variety of clinically relevant paradigms.

Method 1) photochemical crosslinking of a polymer hydrogel matrix followed by oxidative polymerisation of pyrrole yielding poly(ethylene glycol)-chitosan-based hydrogels with an interpenetrating network of polypyrrole (there were partially degradable, as PPY is non-degradable). This type of gels have potential for application as coatings for medical devices where a potential difference could be applied to the coating to release a drug on demand.

Method 2) in-situ crosslinking hydrogels composed of a mixture of chitosan and oxidised hyaluronic acid and water soluble amine displaying poly(3,4-ethylenedioxythiophene) derivatives (there were partially degradable, as the molecular weight of the PEDOT derivatives were not straightforward to characterise). This type of gels have potential to be injected in patient-specific tissue cavities, potentially enabling the simultaneous delivery of drugs and cells to enhance tissue regeneration.

The materials produced by both methodologies were characterised using a variety of techniques readily available at Lancaster University (including FTIR, NMR, XRD, UV-vis, TGA and DSC).

The use of electrically triggered drug delivery from systems produced by method 1 was demonstrated in vitro , whereas the gels produced by method 2 were still in the process of optimisation for their mechanical properties during the project. The data generated with gels produced by methods 1 and 2 have de-risked further investment of time and effort in the generation of families of hydrogels with varying physicochemical properties (mechanics, mesh size, conductivity, etc.) for potential use in drug delivery.

Future Work

Future work for method 1) generating fully biodegradable gels by using water soluble conducting polymers with molecular weights below the renal filtration limit (70 kDa).

Future work for method 2) generating fully biodegradable gels by generating PEDOT derivatives that are renally clearable (i.e. MW below 70 kDa).

Future work for both methods: screen molecular weights of drugs that can be delivered (e.g. low molecular weight drugs, peptides, proteins, DNA, etc.).

We conclude that electroactive hydrogels have great potential for a variety of biomedical applications.